RESEARCH ARTICLE

Gsx2 is required for specification of neurons in the inferior olivary nuclei from Ptf1a-expressing neural progenitors in zebrafish

Tsubasa Itoh[1], Miki Takeuchi[2], Marina Sakagami[1], Kazuhide Asakawa[3], Kenta Sumiyama[4], Koichi Kawakami[3], Takashi Shimizu[1,2] and Masahiko Hibi[1,2,*]

ABSTRACT

Neurons in the inferior olivary nuclei (IO neurons) send climbing fibers to Purkinje cells to elicit functions of the cerebellum. IO neurons and Purkinje cells are derived from neural progenitors expressing the proneural gene *ptf1a*. In this study, we found that the homeobox gene *gsx2* was co-expressed with *ptf1a* in IO progenitors in zebrafish. Both *gsx2* and *ptf1a* zebrafish mutants showed a strong reduction or loss of IO neurons. The expression of *ptf1a* was not affected in *gsx2* mutants, and vice versa. In IO progenitors, the *ptf1a* mutation increased apoptosis whereas the *gsx2* mutation did not, suggesting that *ptf1a* and *gsx2* are regulated independently of each other and have distinct roles. The fibroblast growth factors (Fgf) 3 and 8a, and retinoic acid signals negatively and positively, respectively, regulated *gsx2* expression and thereby the development of IO neurons. *mafba* and Hox genes are at least partly involved in the Fgf- and retinoic acid-dependent regulation of IO neuronal development. Our results indicate that *gsx2* mediates the rostro-caudal positional signals to specify the identity of IO neurons from *ptf1a*-expressing neural progenitors.

KEY WORDS: Gsx2, Ptf1a, Cerebellum, Inferior olivary nuclei, Climbing fibers, Zebrafish

INTRODUCTION

In an initial step during the formation of neural circuits, neurons are differentiated from their neural/neuronal progenitors. The fate of neurons is thought to be determined by inductive signals that their progenitors receive depending on the position of the neural/neuronal progenitors. By receiving positional signals, neural progenitors express transcription factors, such as basic helix-loop-helix (bHLH) and homeobox transcription factors, that function in the differentiation and specification of neurons. Elucidation of these transcription factors and their regulation is a prerequisite for understanding the mechanism of neural circuit formation. Cerebellar neural circuits provide a good model for revealing positional signal-dependent neurogenesis.

In both mammals and teleosts, such as zebrafish, cerebellar neural circuits are composed of several types of neurons, including granule cells (GCs) and Purkinje cells (PCs) in the cerebellum, as well as neurons in the inferior olivary nuclei (IO neurons) in the caudal hindbrain. PCs receive axons from GCs (parallel fibers) and IO neurons (climbing fibers: CFs), then integrate the input information to elicit the functions of the cerebellum. PCs then send output to the outside of the cerebellum via efferent neurons, which are eurydendroid cells in zebrafish. In zebrafish, some GCs also project their axons to dendrites of crest cells, which are PC-like cells located in the medial octavolateral nucleus (MON) of the dorsal hindbrain (Bae et al., 2009; Hashimoto and Hibi, 2012; Hibi and Shimizu, 2012). These neurons are derived from the hindbrain, which contains seven compartments collectively referred to as the rhombomeres (r). PCs and IO neurons are generated from neural progenitors in the dorsal ventricular zone of the hindbrain. Analyses of mutants and cell lineage tracing for the bHLH-type proneural gene pancreas transcription factor 1a (*Ptf1a*) in mice revealed that PCs and IO neurons are derived from *Ptf1a*-expressing progenitors and that *Ptf1a* is required for the generation of these neurons in mice (Hoshino et al., 2005; Yamada et al., 2007). Lineage tracing with transgenic (Tg) zebrafish also showed that PCs and IO neurons are derived from *ptf1a*-expressing (*ptf1a*⁺) progenitors in zebrafish (Kani et al., 2010). Inhibitory neurons in the dorsal cochlear nuclei (DCN neurons) were also shown to be derived from *Ptf1a*⁺ neural progenitor cells in r2-5 in mice (Fujiyama et al., 2009). These reports indicate that, despite being present in the dorsal ventricular zone of all rhombomeres, *ptf1a*⁺ progenitors generate different types of neurons depending on their position. At r1, PCs are generated from *ptf1a*⁺ progenitors and migrate dorsally, whereas in the caudal hindbrain, IO neurons are generated from *ptf1a*⁺ progenitors and migrate ventrally (reviewed by Hashimoto and Hibi, 2012; Hoshino, 2012). However, it is not clear yet how positional signals are interpreted to specify neurons from *ptf1a*⁺ progenitors and what molecules control the differentiation and/or specification of IO neurons.

Rostro-caudal patterning of the caudal hindbrain is controlled by gradients of fibroblast growth factors 3 and 8a (Fgf3/8a) and retinoic acid (RA) signals (Dupé and Lumsden, 2001; Gavalas and Krumlauf, 2000; Marin and Charnay, 2000; Maves et al., 2002; Maves and Kimmel, 2005). During early neurogenesis in zebrafish, *fgf3* and *fgf8a* are expressed at r4 and are required for fate determination of r5 and r6 (Maves et al., 2002; Shimizu et al., 2006; Walshe et al., 2002; Wiellette and Sive, 2004). In the aldehyde dehydrogenase 1 family, the A2 gene (*aldh1a2*) encodes an enzyme that is required for the production of RA and is expressed in forming somites during early neurogenesis (Begemann et al., 2001; Grandel et al., 2002). RA signaling is required for the formation of r5-7 and the anterior spinal cord (Begemann et al., 2001; Grandel et al., 2002; Niederreither et al., 2000; Shimizu et al., 2006). These data suggest that Fgf and RA signal gradients in which Fgf and RA signals are high at r4 and in the caudal-most hindbrain, respectively, play important roles in specifying neurons in the caudal hindbrain. Although Fgf and RA signals regulate the expression of *mafba*, *knox20* and Hox cluster

[1]Division of Biological Science, Graduate School of Science, Nagoya University, Furo, Chikusa, Nagoya, Aichi 464-8602, Japan. [2]Bioscience and Biotechnology Center, Nagoya University, Furo, Chikusa, Nagoya, Aichi 464-8601, Japan. [3]Laboratory of Molecular and Developmental Biology, National Institute of Genetics, Department of Genetics, SOKENDAI (The Graduate University for Advanced Studies), Mishima, 411-8540, Japan. [4]RIKEN Center for Biosystems Dynamics Research (BDR), Suita, Osaka 565-0871, Japan.

*Author for correspondence (hibi@bio.nagoya-u.ac.jp)

M.T., 0000-0002-0726-3415; K.S., 0000-0001-8785-5439; M.H., 0000-0002-9142-4444

DEVELOPMENT

1

genes (Ghosh et al., 2018; Marin and Charnay, 2000; Walshe et al., 2002), it is largely unknown which genes function downstream of these signals to regulate neuronal specification.

In mice, the homeobox gene *Gsx2* (formerly *Gsh2*) is expressed in the ventral telencephalon and is involved in fate determination of lateral ganglionic eminence (LGE) progenitor cells, which give rise to striatal neurons and olfactory bulb interneurons (Corbin et al., 2000; Hsieh-Li et al., 1995; Szucsik et al., 1997; Waclaw et al., 2009; Yun et al., 2003). *Gsx2*, which is also expressed in the ventricular zone of the spinal cord and hindbrain, is involved in the generation of a subset of hindbrain neurons and dorsal interneurons in the spinal cord of mice (Kriks et al., 2005; Mizuguchi et al., 2006; Satou et al., 2013). However, the role of *gsx2* in the development of IO neurons has not been elucidated. In this report, we show that *gsx2* is co-expressed with *ptf1a* in neuronal progenitors of IO neurons and is required for the development of IO neurons in zebrafish. *gsx2* expression is regulated through transcriptional networks that are activated by Fgf and RA signals in the caudal hindbrain. Our results reveal that *gsx2* mediates the rostro-caudal positional signals to control the identity of IO neurons.

RESULTS

gsx2 is co-expressed in IO progenitors that express *ptf1a*

To reveal the mechanisms that generate IO neurons, we sought genes that are expressed in IO progenitors in the dorso-caudal hindbrain. A previous study with a BAC transgenic fish *TgBAC(gsx2:LOXP-Tomato-LOXP-GFP)* [hereafter referred to as *Tg(gsx2:RFP)*] suggested that *gsx2* is expressed in the caudal hindbrain (Satou et al., 2013). Thus, we focused on *gsx2* and *ptf1a*, which is also involved in the generation of IO neurons in mice (Yamada et al., 2007). We found that *gsx2* was expressed in the dorsal part of the caudal hindbrain and the ventral telencephalon in an early stage [2, 3 days post fertilization (dpf)] of zebrafish larvae (Fig. 1A,B,E,F). As reported previously, *ptf1a* was expressed in the dorsal ventricular zone of all rhombomeres (Fig. 1C,D,G,H). To examine *gsx2*-expressing cells in detail, we compared RFP expression in *Tg(gsx2:RFP)* larvae (gsx2:RFP) with GFP expression in gSAIzGFFM35A; *Tg(5xUAS:EGFP)* (Fig. 1I-L) and *Tg(ptf1a:EGFP)* larvae (ptf1a:GFP, Fig. 1M-W). gSAIzGFFM35A is a Gal4 trap line that harbors a Gal4 gene in the exon of *mafba* (previously known as *valentino* or *kreisler*) and can drive UAS-mediated GFP expression at r5 and 6 (referred to as mafba^GFF;UAS:GFP, Fig. 1I,K) (Asakawa and Kawakami, 2018). The gsx2:RFP^+ and mafba^GFF;UAS:GFP^+ cells did not overlap and were separated adjacently in the caudal hindbrain at an early larval stage (3 dpf, Fig. 1I-L), indicating that *gsx2* is specifically expressed in r7 of the hindbrain and the rostral spinal cord. As reported previously (Kani et al., 2010), ptf1a:GFP expression was detected in neural progenitors located in the dorsal ventricular zone of all rhombomeres at an early larval stage (5 dpf, Fig. 1M,N, Q). gsx2:RFP expression was detected in the dorsal ventricular zone of only the caudal hindbrain (Fig. 1M,O,Q). gsx2:RFP and ptf1a: GFP were co-expressed in cells in the dorsal ventricular zone (Fig. 1M,Q). As GFP and RFP (Tomato) are relatively stable, they can be used for lineage tracing in zebrafish (Kani et al., 2010). Although *gsx2* and *ptf1a* were not detected in the ventral hindbrain (Fig. 1E-H), gsx2:RFP and ptf1a:GFP were co-expressed in neurons in the ventral hindbrain in 5-dpf larvae (Fig. 1R-T). The gsx2:RFP^+ neurons in the ventral hindbrain projected their axons to the cerebellum (Fig. 1O,P,V,W). To examine whether they are IO neurons, we used the Tg line hspGFFDMC28C;*Tg(5xUAS:EGFP)* (28C;UAS:GFP), which expresses GFP in IO neurons (Takeuchi et al., 2015). gsx2:RFP and 28C;UAS:GFP were co-expressed in
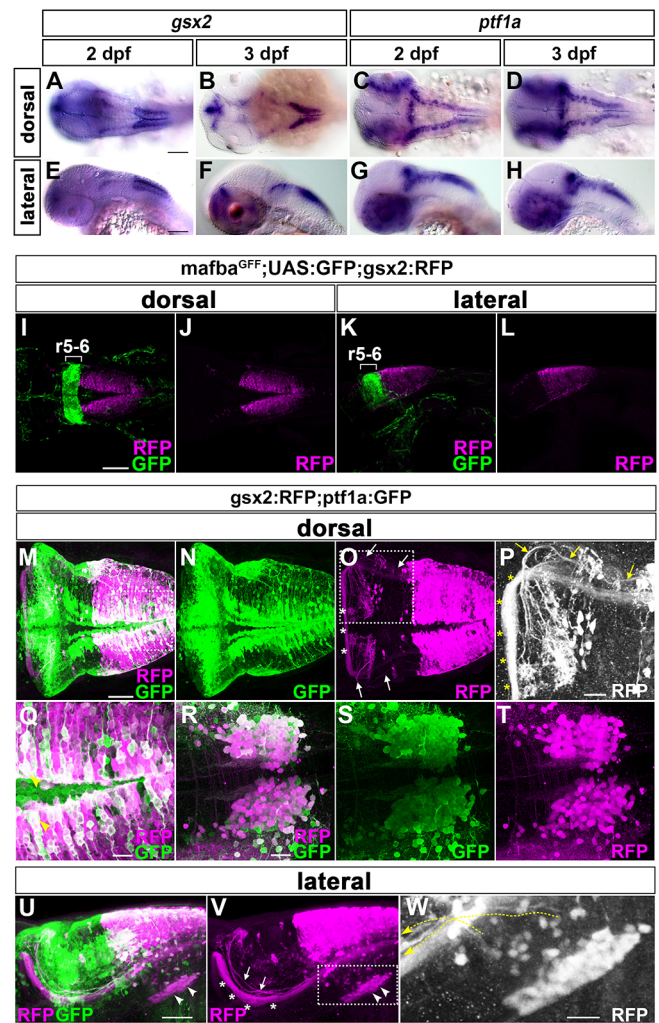

Fig. 1. *gsx2* and *ptf1a* are co-expressed in IO progenitors.
(A,B,E,F) Expression of *gsx2* in 2 and 3 dpf larvae. (C,D,G,H) Expression of *ptf1a* in 2 and 3 dpf larvae. (I-L) 3 dpf mafba^GFF;UAS:GFP;gsx2:RFP larvae (*n*=2) were immunostained using anti-DsRed (RFP, magenta) and anti-GFP (green) antibodies. r5-6, rhombomeres 5 and 6. (M-W) 5 dpf gsx2:RFP;ptf1a: GFP larvae were immunostained using anti-DsRed (magenta) and anti-GFP (green) antibodies. Dorsal views (M-T) and lateral views (U-W). (P) Higher magnification of the dotted box in O. (Q) Higher magnification of the dotted box in M (dorsal optical section). (R-T) Expression of GFP and/or RFP in the IO region. (W) Higher magnification of the dotted box in V. White and yellow arrows, and white arrowheads indicate CFs and IO neurons, respectively. Yellow arrowheads indicate both GFP^+ and RFP^+ cells. Asterisks indicate gsx2:RFP^+ axons that are potentially axons from the nucleus commissure of Wallenberg, which sends mossy fibers projecting to GCs. Dotted yellow arrows in W indicate axons from IO neurons. Scale bars: 100 μm in A,E (apply to A-H) and I (applies to I-L); 50 μm in M (applies to M-O) and U (applies to U,V); 20 μm in P-R (bar in R applies to R-T) and W.

neurons in the ventral part of the caudal hindbrain (Fig. S2). Although there were gsx2:RFP^+ 28C;UAS:GFP^− cells in this region (Fig. S2), the absence of 28C;UAS:GFP expression may be due to a mosaic expression of UAS:GFP (Akitake et al., 2011). These results indicate that *gsx2* is co-expressed with *ptf1a* in IO progenitors. We also found that gsx2:RFP^+ axons from the ventro-lateral part of the caudal hindbrain projected to the ventral part of the cerebellum (Fig. 1O,P). These axons are potentially from the nucleus commissure of Wallenberg, which send mossy fibers that project to GCs, as reported for other teleost species (Xue et al., 2004).

The *gsx2* mutation leads to a strong reduction or loss of IO neurons

To reveal the roles of Gsx2 in IO neuronal development, we generated *gsx2* mutants using the CRISPR/Cas9 method. The *gsx2* mutants harbor a 5 bp ($gsx2^{\Delta 5}$) or 8 bp ($gsx2^{\Delta 8}$) deletion in exon 1 of the *gsx2* gene that introduces a premature stop (Fig. S1). Although *gsx2* mRNA was not reduced in the *gsx2* mutant larvae (Fig. S3), the Gsx2 proteins of the putative mutants lack the homeodomain (Fig. S1) and the mutations are likely null alleles. In control 5 dpf 28C;UAS:GFP Tg larvae, GFP+ somata were located in the ventral hindbrain and they extended CFs to PCs, which were marked with anti-parvalbumin7 (Pvalb7) antibody (Fig. 2A-D, Fig. S4). In contrast, GFP+ somata were rarely detected and GFP+ CFs were not observed in *gsx2* mutants (Fig. 2E-H,M, Fig. S4). In addition to 28C;UAS:GFP, we found that the *TgBAC(mnx2b:GFF);Tg(5xUAS:EGFP)* line also expressed GFP in a region of IO neurons in addition to motoneurons (mnx2b:GFF; UAS:GFP) (Asakawa et al., 2013) (Fig. 2I,J). mnx2b:GFF;UAS:GFP and gsx2:RFP were co-expressed in neurons in the ventral part of the caudal hindbrain (Fig. S2). Similar to 28C;UAS:GFP+ cells, a strong reduction or loss of mnx2b:GFF;UAS:GFP+ IO neurons was observed in 5 dpf $gsx2^{\Delta 5}$ mutant larvae (Fig. 2K,L). We further examined endogenous markers of IO neurons. *pou4f1* (also known as *brn3a*) and a glutamate receptor, metabotropic 5a (*grm5a*), are expressed in

zebrafish IO neurons (Bae et al., 2009; Haug et al., 2013). *foxp2* is expressed in IO neurons of mice (Ferland et al., 2003; Fujita and Sugihara, 2012). Whereas the expression of these markers was detected in IO neurons of wild-type larvae, it was not observed in *gsx2* mutant larvae (Fig. 2N-S, Fig. S4), indicating a strong reduction or absence of IO neurons in *gsx2* mutants. These data reveal that Gsx2 is required for IO neuronal development (Fig. 2T). In addition, mnx2b: GFF;UAS:GFP+ neurons located in the ventro-lateral part of the caudal hindbrain were reduced or absent in *gsx2* mutants (Fig. 2I,K).

The *ptf1a* mutation leads to a strong reduction or loss of IO neurons

We next analyzed the roles of *ptf1a* in the development of IO neurons by generating *ptf1a* mutants using the CRISPR/Cas9 method. The *ptf1a* mutants have a 4 bp ($ptf1a^{\Delta 4}$) deletion or 11 bp insertion ($ptf1a^{+11}$) in exon 1 (Fig. S1). Although the *ptf1a* mutant larvae retained *ptf1a* mRNA (Fig. S3), the putative mutant Ptf1a proteins lack the bHLH domain and the mutations were likely null alleles. The *ptf1a* mutant larvae displayed a complete loss of IO neurons that express GFP in 28C;UAS:GFP or mnx2b:GFF;UAS: GFP Tg lines (Fig. 3E-H,K-M Fig. S4). Furthermore, the IO markers *pou4f1*, *grm5a* and *foxp2* were not detected in *ptf1a* mutant larvae (Fig. 3N-S, Fig. S4). These results are consistent with the
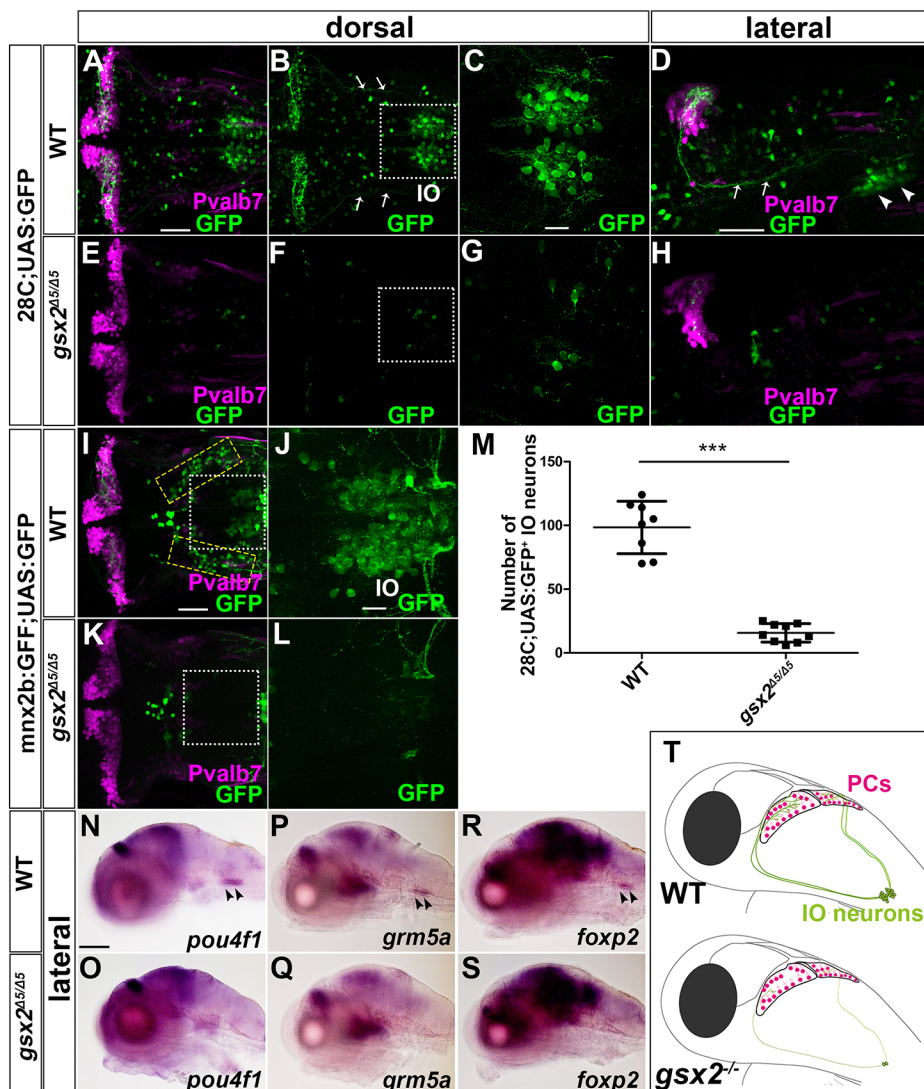

Fig. 2. Strong reduction or loss of IO neurons in *gsx2* mutants. (A-H) 5 dpf wild-type (A-D, *n*=10) and $gsx2^{\Delta 5/\Delta 5}$ (E-H, *n*=10) hspGFFDMC28C;UAS:GFP (28C;UAS:GFP) larvae immunostained using anti-Pvalb7 (magenta) and anti-GFP (green) antibodies. Arrows and arrowheads indicate CFs and IO neurons, respectively. (C,G) Higher magnification of the boxes in B and F. (I-L) 5 dpf wild-type (I,J, *n*=6) and $gsx2^{\Delta 5/\Delta 5}$ (K,L, *n*=7) mnx2b:GFF;UAS:GFP larvae. GFP+ cells in the yellow dotted boxes were fewer or absent in $gsx2^{\Delta 5/\Delta 5}$ larvae. (J,L) Higher magnification of the boxes in I and K. (M) Number of 28C;UAS: GFP+ IO neurons in wild-type and $gsx2^{\Delta 5/\Delta 5}$ larvae. 28C;UAS:GFP+ IO neurons were significantly fewer in *gsx2* mutant larvae compared with control larvae. ***P<0.001 (Student's *t*-test). Data are mean±s.e.m. with individual values indicated. (N-S) Expression of endogenous IO neuronal markers in wild type and $gsx2^{\Delta 5/\Delta 5}$. (N,O) Expression of *pou4f1* in wild type (*n*=4) and $gsx2^{\Delta 5/\Delta 5}$ (*n*=4). (P,Q) Expression of *grm5a* in wild type (*n*=3) and $gsx2^{\Delta 5/\Delta 5}$ (*n*=2). (R,S) Expression of *foxp2* in wild type (*n*=5) and $gsx2^{\Delta 5/\Delta 5}$ (*n*=5). (T) Illustration of PCs and IO neurons in wild-type and *gsx2* mutant larvae. Scale bars: 100 μm in N (applies to N-S); 50 μm in A (applies to A,B,E,F), D (applies to D,H) and I (applies to I, K); 20 μm in C (applies to C,G) and J (applies to J,L).
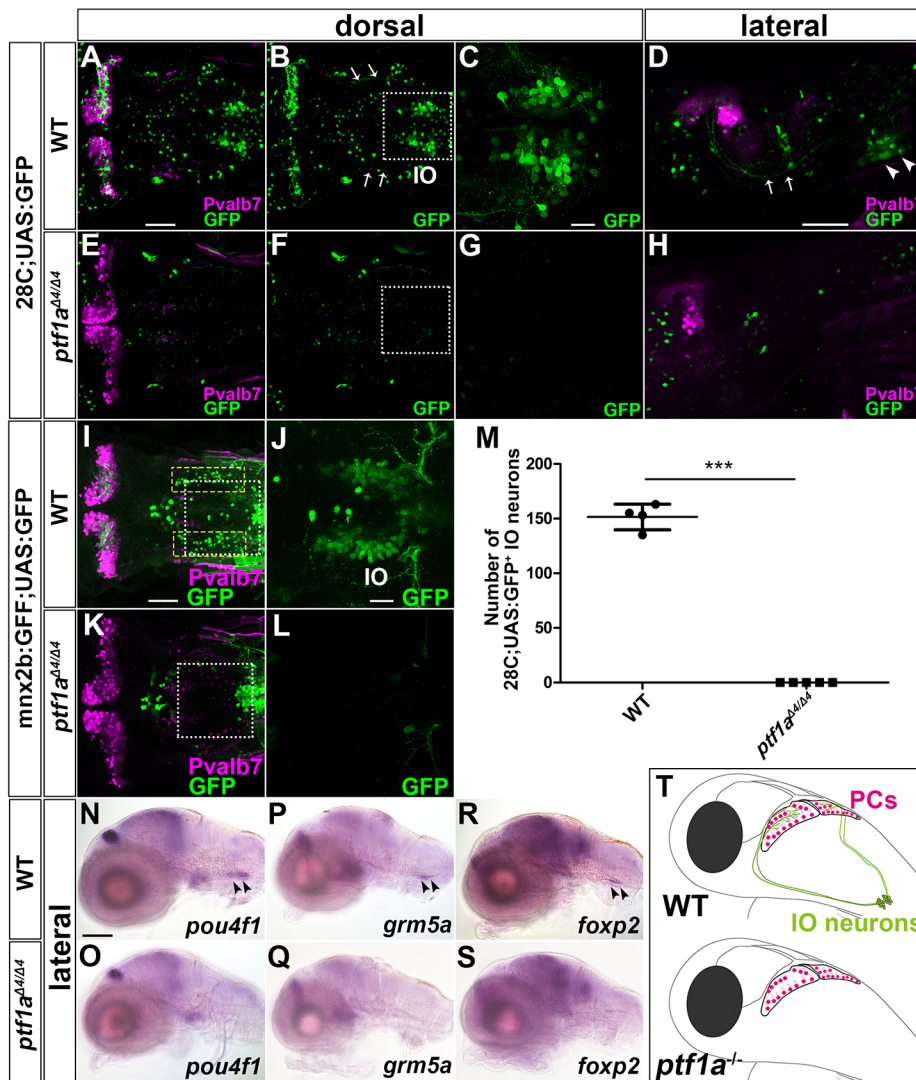
Fig. 3. Loss of IO neurons in *ptf1a* mutants. (A-H) 5 dpf wild-type (A-D, *n*=5) and *ptf1a*$^{Δ4/Δ4}$ (E-H, *n*=5) 28C;UAS:GFP larvae were immunostained using anti-Pvalb7 (magenta) and anti-GFP (green) antibodies. Arrows and arrowheads indicate CFs and IO neurons, respectively. (C,G) Higher magnification of the boxes in B and F. (I-L) 5 dpf wild-type (I-J *n*=2) and *ptf1a*$^{Δ4/Δ4}$ (K-L *n*=4) mnx2b:GFF;UAS:GFP larvae. GFP$^+$ cells in the yellow dotted boxes were fewer or absent in *ptf1a*$^{Δ4/Δ4}$ larvae. (J,L) Higher magnification of the boxes in I and K. (M) Number of 28C;UAS:GFP$^+$ IO neurons in wild-type and *ptf1a*$^{Δ4/Δ4}$ larvae. 28C;UAS:GFP$^+$ IO neurons were significantly reduced in *ptf1a* mutant larvae compared with control larvae. ***$P<0.001$ (Student's *t*-test). Data are mean± s.e.m. with individual values indicated. (N,O) Expression of pou4f1 in 5 dpf wild-type (*n*=4) and *ptf1a*$^{Δ4/Δ4}$ (*n*=4) larvae. (P,Q) Expression of grm5a in 5 dpf wild-type (*n*=4) and *ptf1a*$^{Δ4/Δ4}$ (*n*=3) larvae. (R,S) Expression of foxp2 in 5 dpf wild-type (*n*=5) and *ptf1a*$^{Δ4/Δ4}$ (*n*=5) larvae. (T) Illustration of Purkinje cells and IO neurons in wild-type and *ptf1a* mutant larvae. Scale bars: 100 µm in N (applies to N-S); 50 µm in A (applies to A,B,E,F), D (applies to D,H) and I (applies to I,K); 20 µm in C (applies to C,G) and J (applies to J,L).

defective development of IO neurons in *Ptf1a* mutant mice (Yamada et al., 2007). In addition to IO neurons, the *ptf1a* mutants showed a reduction or loss of mnx2b:GFF;UA:GFP$^+$ neurons in the ventro-lateral hindbrain as in *gsx2* mutants (Fig. 3K,L). Currently, the identity of these neurons is not known, but they are likely derived from *gsx2*- and *ptf1a*-expressing neural progenitors. The *ptf1a* mutants further displayed a reduction – but not loss – of PCs and crest cells, which were positive for Pvalb7, as was shown previously (Bae et al., 2009) (Fig. 3E, Fig. S5). These data suggest that, even though PCs, crest cells and IO neurons are derived from *ptf1a*-expressing progenitors, *ptf1a* functions redundantly with other genes during the development of PCs and crest cells, while *ptf1a* is essential for the development of IO neurons in zebrafish (Fig. 3T).

Non-interdependent regulation and distinct roles of *gsx2* and *ptf1a* in IO progenitors

We examined the relationship between *gsx2* and *ptf1a* in IO neuronal development. The expression of *ptf1a* and *gsx2* was not affected in *gsx2* and *ptf1a* mutant larvae, respectively, during the development of IO neurons (Fig. 4). These results indicate that *ptf1a* and *gsx2* are regulated independently of each other in the caudal hindbrain. We further analyzed apoptosis by immunohistochemistry with an anti-

cleaved caspase 3 antibody as *Ptf1a* mouse mutants show an increase in apoptotic cells in the caudal hindbrain (Yamada et al., 2007). As in *Ptf1a* mutant mice, the *ptf1a* zebrafish mutant larvae showed an increase in the number of cleaved-caspase 3$^+$ cells (Fig. 5A-H,Q). In contrast, there was no significant increase in cleaved-caspase 3$^+$ cells in *gsx2* mutant larvae (Fig. 5I-P,R). Furthermore, gsx2:RFP
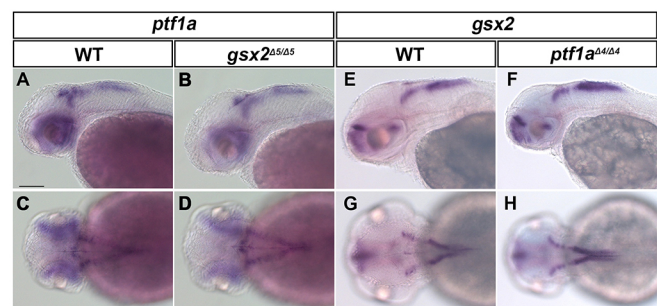

Fig. 4. Expression of *ptf1a* and *gsx2* was not affected in *gsx2* and *ptf1a* mutants. (A-D) Expression of *ptf1a* in 2-dpf wild-type (A,C, *n*=2) and *gsx2* mutant (B,D, *n*=4) larvae. (E-H) Expression of *gsx2* in 2 dpf wild-type (E,G, *n*=2) and *ptf1a* mutant (F,H, *n*=3) larvae. Scale bars: 100 µm in A (applies to A, B,E,F) and C (applies to C,D,G,H).
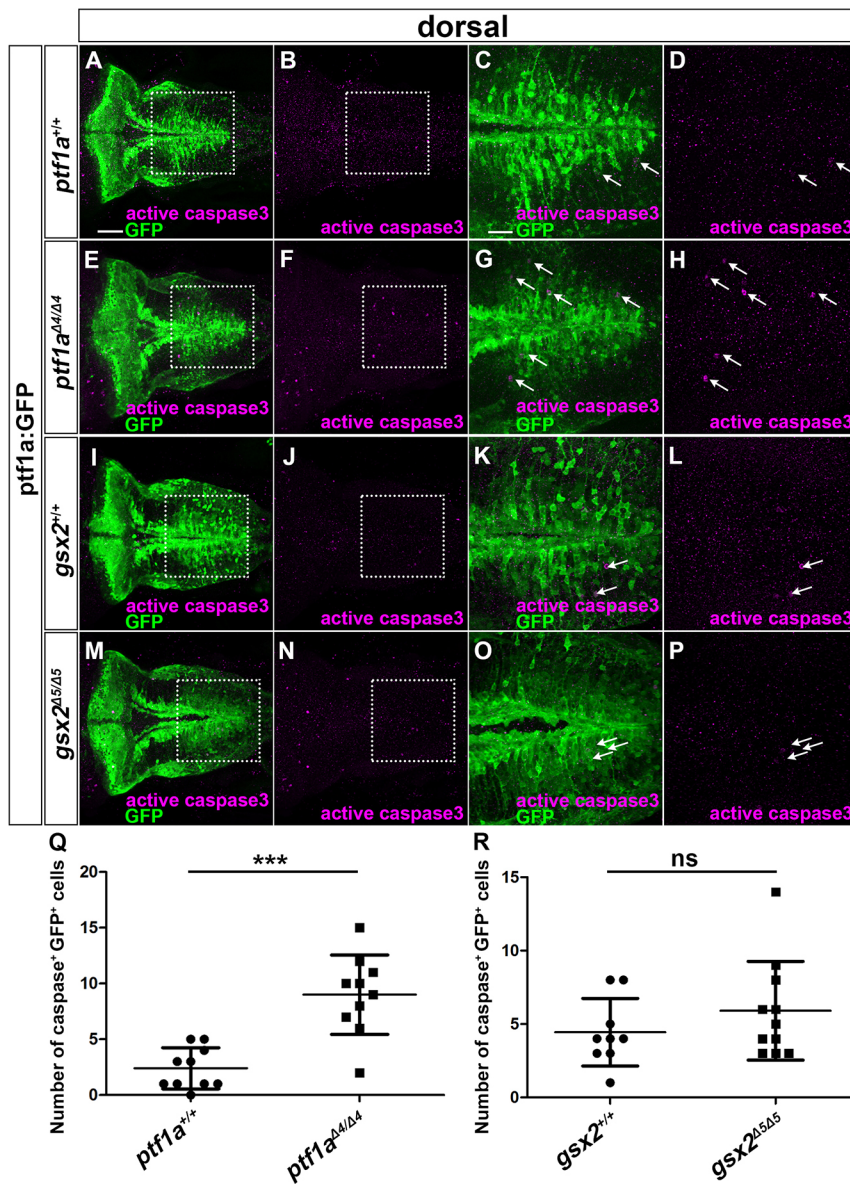
Fig. 5. Apoptosis occurs in *ptf1a* but not *gsx2* mutants. (A-P) 5 dpf *ptf1a*$^{+/+}$ (A-D, n=10), *ptf1a*$^{\Delta4/\Delta4}$ (E-H, n=10), *gsx2*$^{+/+}$ (I-L, n=9) and *gsx2*$^{\Delta5/\Delta5}$ (M-P, n=11) ptf1a:GFP larvae were stained using anti-GFP (green) and anti-cleaved caspase 3 (magenta) antibodies. (C,G, K,O) Higher magnification of the boxes in A,E,I,M. (D,H,L, P) Higher magnification of the boxes in B,F,J,N. Arrows indicate both GFP$^+$ and cleaved caspase 3$^+$ cells. (Q,R) Number of GFP$^+$ and cleaved caspase 3$^+$ cells in the caudal hindbrain in wild type, and the *ptf1a* and *gsx2* mutants. ns, not significant; ***P<0.001 (Student's *t*-test for Q,R). Data are mean±s.e.m. with individual values indicated. Scale bars: 50 µm in A (applies to A,B,E,F,I,J, M,N); 20 µm in C (applies to C,D,G,H,K,L,O,P).

expression was retained in cells migrating from the dorsal progenitor domain in *gsx2* mutant larvae (Fig. S6), suggesting that *gsx2*$^+$ progenitors remained undifferentiated, or differentiated into other neurons in *gsx2* mutants. Our findings indicate that *ptf1a* and *gsx2* play different roles in IO neuronal development.

To further address the cooperative role between *ptf1a* and *gsx2* in IO neuronal development, we expressed *gsx2* in *ptf1a*-expressing progenitors by using ptf1a:Gal4-VP16 and UAS:gsx2 Tg lines (Fig. 6B,C,E,G). However, the ectopic co-expression of *ptf1a* and *gsx2* did not induce ectopic IO neurons in the rostral hindbrain. These data indicate that co-expression of *ptf1a* and *gsx2* is not sufficient to induce IO neurons in the hindbrain.

gsx2 expression is negatively regulated by Fgf signaling and Mafba

Gradients of Fgf and RA signals are involved in the formation and patterning of the caudal hindbrain (Dupé and Lumsden, 2001; Gavalas and Krumlauf, 2000; Marin and Charnay, 2000; Maves et al., 2002). We inhibited Fgf and RA signals in order to investigate the regulation of *gsx2* expression. The inhibition of *fgf8a* and *fgf3* by injection of

antisense morpholino (MO) into *fgf8a* mutants (*fgf8a*$^{ti282a/ti282a}$; *fgf3*^{MO}) significantly increased gsx2:RFP expression and the number of 28C;UAS:GFP$^+$ IO neurons, compared with control MO-injected wild-type larvae (Fig. 7A-D,I,K-P,W). Consistent with this finding, inhibition of the Fgf signal by SU5402, which is a chemical inhibitor of Fgf receptor tyrosine kinases (Mohammadi et al., 1997), led to an expansion of gsx2:RFP expression and an increase in the number of 28C;UAS:GFP$^+$ IO neurons (Fig. 7E-H,J,Q-V,X). Stronger Fgf inhibition by SU5402 correlated with an increase in gsx2:RFP expression and IO neurons (Fig. S7). Our findings suggest that the Fgf signal suppressed rostral expansion of *gsx2* expression, thereby limiting the *gsx2*-expressing IO progenitor domain to r7. The expansion of *gsx2* expression by inhibition of the Fgf signal likely led to the expansion of IO progenitors and a subsequent increase in IO neurons.

mafba^{GFF};UAS:GFP expression was reduced when the Fgf signal was inhibited (Fig. 7G,H). We further analyzed the roles of *mafba* in *gsx2* expression and in the development of IO neurons (Fig. 8). In *mafba*$^{GFF/GFF}$ mutant larvae (Asakawa and Kawakami, 2018), rostral gsx2:RFP expression expanded slightly compared with
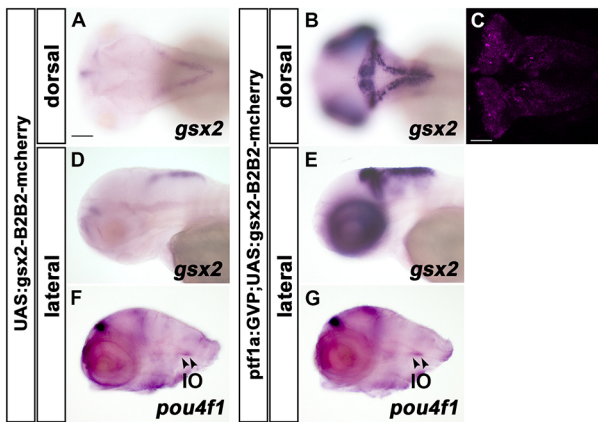
Fig. 6. Ectopic *gsx2* expression alone does not induce IO neurons.
(A,B,D,E) Expression of *gsx2* in 3 dpf *Tg(UAS:gsx2BLRP-P2A-BirA-P2A-mCherry)* (control, A,D, *n*=5) and *TgBAC(ptf1a:Gal4-VP16);Tg(UAS:gsx2BLRP-P2A-BirA-P2A-mCherry)* (B,E, *n*=5) larvae. The *Tg(UAS:gsx2BLRP-P2A-BirA-P2A-mCherry)* line harbors a transgene containing the open reading frame (ORF) of *gsx2*, biotin ligase recognition peptide (BLRP), 2A peptide sequences of porcine teschovirus-1 (P2A), biotin ligase (BirA) and mCherry genes. Expression of Gsx2 and mCherry can be driven by Gal4-VP16. (C) Expression of mCherry was induced where *ptf1a* was expressed in 3 dpf Tg larvae. (F,G) Expression of *pou4f1* in 3 dpf control (F, *n*=3) and *Tg(ptf1a:Gal4-VP16);Tg(UAS:gsx2BLRP-P2A-BirA-P2A-mCherry)* (G, *n*=3) larvae. Although *gsx2* was ectopically expressed in all *ptf1a*-expressing cells, it did not induce ectopic expression of *pou4f1*. Scale bars: 100 μm in A (applies to A,B, D-G); 50 μm in C.

control heterozygotes, and gsx2:RFP^{+} cells were observed in the mafba[GFF];UASGFP[+] region, corresponding to r5/6 (Fig. 8D-F,O). Furthermore, 28C;UAS:GFP^{+} IO neurons increased significantly in *mafba*[b337/b337] mutant larvae (Fig. 8K-N,P). These data suggest that Mafba is at least partly involved in the Fgf signal-mediated suppression of *gsx2* expression and IO neuronal development.

gsx2 expression is positively regulated by the RA-Hox cascade

We inhibited the RA signal by a MO against *aldh1a2*, which recapitulates the phenotypes of an *aldh1a2* mutant (Begemann et al., 2001), or an Aldh1a2 inhibitor diethylaminobezaldehyde (DEAB) (Russo, 1997). Inhibition of the RA signal with both MO and DEAB resulted in reduced gsx2:RFP expression but increased mafba[GFF];UAS:GFP expression (r5/6, Fig. 9A-L). It also reduced the number of 28C;UAS:GFP^{+} IO neurons (Fig. 9M-T,Y,Z) and expression of the IO neuronal marker *pou4f1* (Fig. 9U-X). The reduction was stronger in DEAB-treated larvae than in *aldh1a2* morphants, consistent with a previous report showing that DEAB-treated larvae showed more severe phenotypes than *aldh1a2* mutants (Begemann et al., 2004). Our data indicate that the RA signal positively controls *gsx2* expression in the caudal hindbrain, and is also involved in IO neuronal development. The reduction in *gsx2* expression by inhibition of the RA signal likely led to the reduction of IO progenitors and the subsequent reduction of IO neurons.

The RA signal controls the expression of Hox genes in the caudal hindbrain (Ghosh et al., 2018; Marin and Charnay, 2000). To address the roles of Hox genes in IO neuronal development, we examined *gsx2* expression and IO neurons in larvae defective of Pbx2 and Pbx4, which are co-factors in the rostral Hox protein (Waskiewicz et al., 2002). The *pbx2/pbx4* morphant larvae recapitulate the phenotypes of maternal zygotic *pbx2* mutants in which *pbx4* inhibition was mediated by MO, and in which r2-6
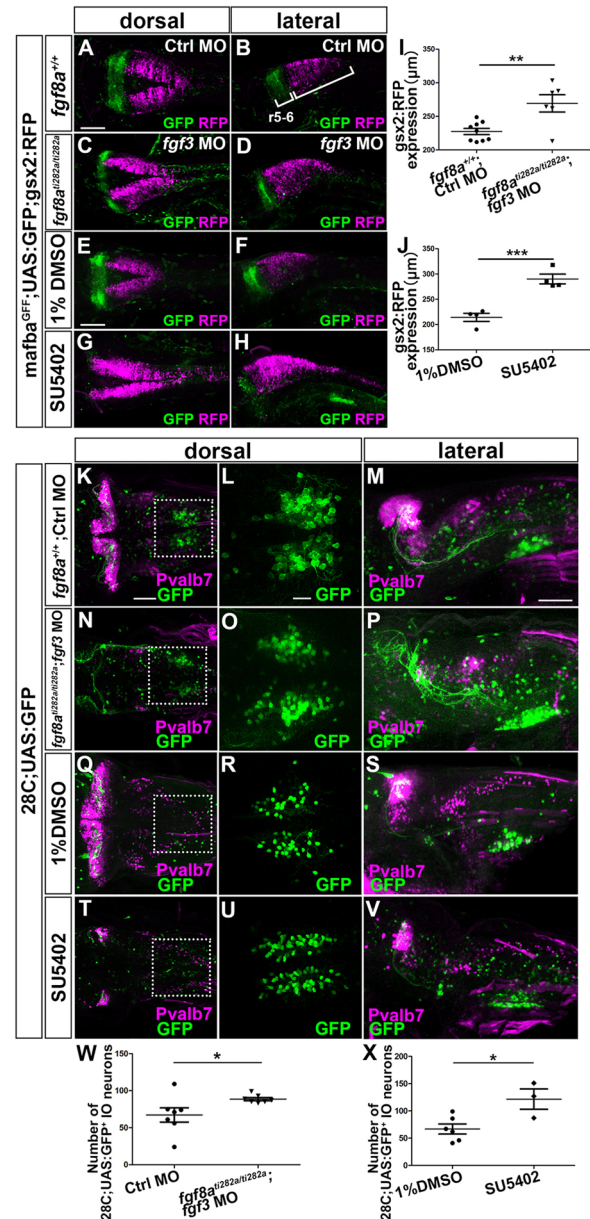

Fig. 7. Fgf signal suppresses *gsx2* expression and IO neuronal development. (A-D) 3 dpf control (*fgf8a*^{+/+}) and *fgf8a*[ti282a/ti282a] mafba[GFF];UAS:GFP;gsx2:RFP larvae that received an injection of control (Ctrl) MO and *fgf3* MO, respectively, were stained using anti-RFP (magenta) and anti-GFP (green) antibodies. (E-H) mafba[GFF];UAS:GFP;gsx2:RFP were treated with 1% DMSO (E,F, *n*=4) or 200 μM SU5402 (G,H, *n*=4) from 6 to 22 hpf, fixed at 3 dpf, and stained using anti-RFP (magenta) and anti-GFP (green) antibodies. (I,J) Length of the gsx2:RFP[+] hindbrain region (*gsx2* expression) in *fgf8a*^{+/+}; Ctrl MO (*n*=9) and *fgf8a*[ti282a/ti282a]; *fgf3*[MO] (*n*=6) larvae (I), and in DMSO- (*n*=4) or 200 μM SU5402-treated (*n*=4) larvae (J). (K-P) Expression of GFP (green) and Pvalb7 (magenta) in control (*fgf8a*^{+/+}) and *fgf8a*[ti282a/ti282a] 28C;UAS:GFP larvae that received an injection of control MO and *fgf3* MO (*fgf3*[MO]), respectively. (Q-V) 28C;UAS:GFP were treated with 1% DMSO (Q-S, *n*=6) or 5.0 μM SU5402 (T-V, *n*=3) from 6 to 22 hpf, fixed at 3 dpf, and stained using anti-Pvalb7 (magenta) and anti-GFP (green) antibodies. (L,O,R,U) Higher magnification of the boxes in K,N,Q,T. (W) Number of 28C;UAS:GFP^{+} IO neurons in *fgf8a*^{+/+};Ctrl MO (*n*=6) and *fgf8a*[ti282a/ti282a]; *fgf3* MO (*n*=5) larvae. (X) Number of 28C;UAS:GFP^{+} IO neurons in DMSO- (*n*=6) or 5.0 μM SU5402-treated (*n*=3) larvae. r5-6, rhombomeres 5 and 6. *$P<0.05$; **$P<0.01$; ***$P<0.001$ (Student's *t*-test for J and X, Welch's *t*-test for I and W). Data are mean±s.e.m. with individual values indicated. Scale bars: 100 μm in A (applies to A-D) and E (applies to E-H); 50 μm in K (applies to K,N,Q,T) and M (applies to M,P,S,V); 20 μm in L (applies to L,O,R,U).

6

acquired the r1 state (Maves et al., 2009). In *pbx2/4* morphant larvae, ectopic PCs were observed caudally but crest cells were present normally (Fig. 10G). In contrast, gsx2:RFP expression, the number of 28C;UAS:GFP⁺ IO neurons (determined by their location in the caudal hindbrain and their axons) and *pou4f1* expression were strongly reduced or absent in *pbx2/4*-deficient larvae (Fig. 10C,D,G,H,J,K,L). To address the roles of Hox genes, we further ectopically expressed *hoxb4a* as it is expressed in r7 and in the spinal cord. Injection of *hoxb4a* mRNA expanded gsx2:RFP expression and increased 28C;UAS:GFP⁺ IO neurons in the caudal hindbrain (Fig. 10O-R). Furthermore, injection of *hoxb4a* mRNA at least partly rescued gsx2:RFP expression and 28C;UAS:GFP⁺ IO neurons in *aldh1a2* morphants or DEAB-treated larvae (Fig. 10S-V). Although *hoxb4a* might not be the only Hox gene regulating caudal-most hindbrain identity, our data suggest that the RA-Hox cascade plays a major role in controlling *gsx2* expression and subsequent IO neuronal development.

DISCUSSION
Expression of *gsx2* and *ptf1a* in IO progenitors located in rhombomere 7
gsx2 and *ptf1a* were expressed in the dorsal ventricular zone of r7 (Fig. 1). Tracing with the Tg lines revealed that *gsx2*- and *ptf1a*-expressing cells (gsx2:RFP⁺ and ptf1a:GFP⁺ cells) gave rise to IO

neurons (Fig. 1). Consistent with this, single-cell RNA sequencing analysis revealed that *gsx2* and *ptf1a* were co-expressed in dorsomedial progenitor cells of the hindbrain (Tambalo et al., 2020). Furthermore, the *gsx2* and *ptf1a* mutations abrogated IO neuronal development (Figs 2 and 3). These data indicate that *gsx2/ptf1a*-expressing cells are the neural progenitors of IO neurons. Previous lineage tracing with the Cre-loxP system in mice revealed that IO neurons were derived from *Ptf1a*-expressing neural progenitors (Yamada et al., 2007). Avian grafting studies suggested that IO neural progenitors were located in r6-8 (Ambrosiani et al., 1996; Cambronero and Puelles, 2000; Kawauchi et al., 2006). Our data clearly indicate that, in zebrafish, IO neurons are derived from *gsx2/ptf1a*-expressing neural progenitors in r7.

Role of Ptf1a in the development of hindbrain neurons
ptf1a (*Ptf1a* in mice) is expressed in neural progenitors in the ventricular zone of the entire dorsal hindbrain in both mice and zebrafish (Fujiyama et al., 2009; Hoshino et al., 2005; Kani et al., 2010; Yamada et al., 2007). Zebrafish *ptf1a* mutants showed a reduction in the number of PCs and crest cells, and the loss of IO neurons (Fig. 3, Fig. S5). In mice, *Ptf1a* mutants showed a complete loss of PCs (and other cerebellar GABAergic interneurons), DCN neurons and IO neurons (Fujiyama et al., 2009; Hoshino et al., 2005;
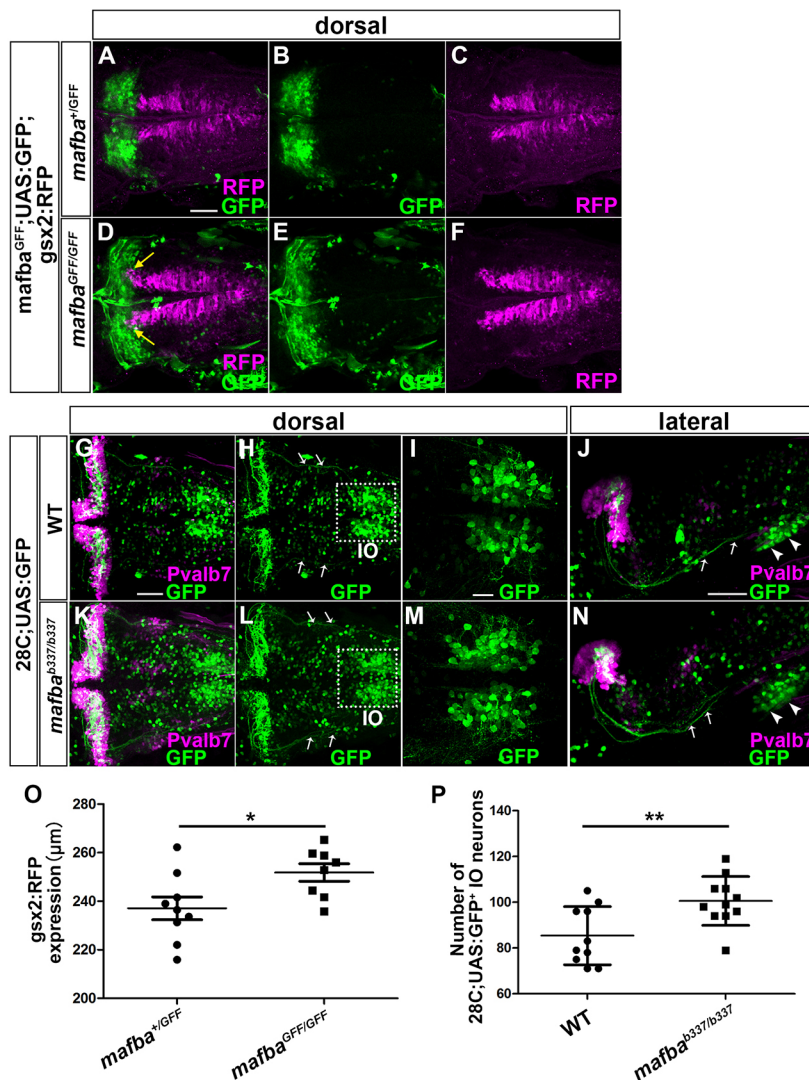

Fig. 8. Mafba negatively controls *gsx2* expression and IO neuronal development. (A-F) 3-dpf *mafba*⁺/GFF (A-C, *n*=9) and *mafba*GFF/GFF (D-F, *n*=8);UAS:GFP;gsx2:RFP larvae were stained with anti-RFP (magenta) and anti-GFP (green) antibodies. Yellow arrows indicate that *gsx2* expression extends to rhombomeres 5 and 6. (G-N) 5-dpf wild-type (G-J, *n*=10) and *mafba*b337/b337 28C;UAS:GFP (K-N, *n*=11) larvae were stained with anti-GFP (green) and anti-Pvalb7 (magenta) antibodies. Arrows and arrowheads indicate CFs and IO neurons, respectively. (O) Length of gsx2:RFP⁺ hindbrain region in *mafba*⁺/GFF and *mafba*GFF/GFF. (P) Number of 28C;UAS:GFP⁺ IO neurons in wild-type and *mafba*b337/b337 larvae. *P<0.05; **P<0.01 (Student's *t*-test). Data are mean± s.e.m. with individual values indicated. Scale bars: 50 µm in A (applies A to F) and G (applies to G,H,K,L) and J (applies to J, N); 20 µm in I (applies to I,M).
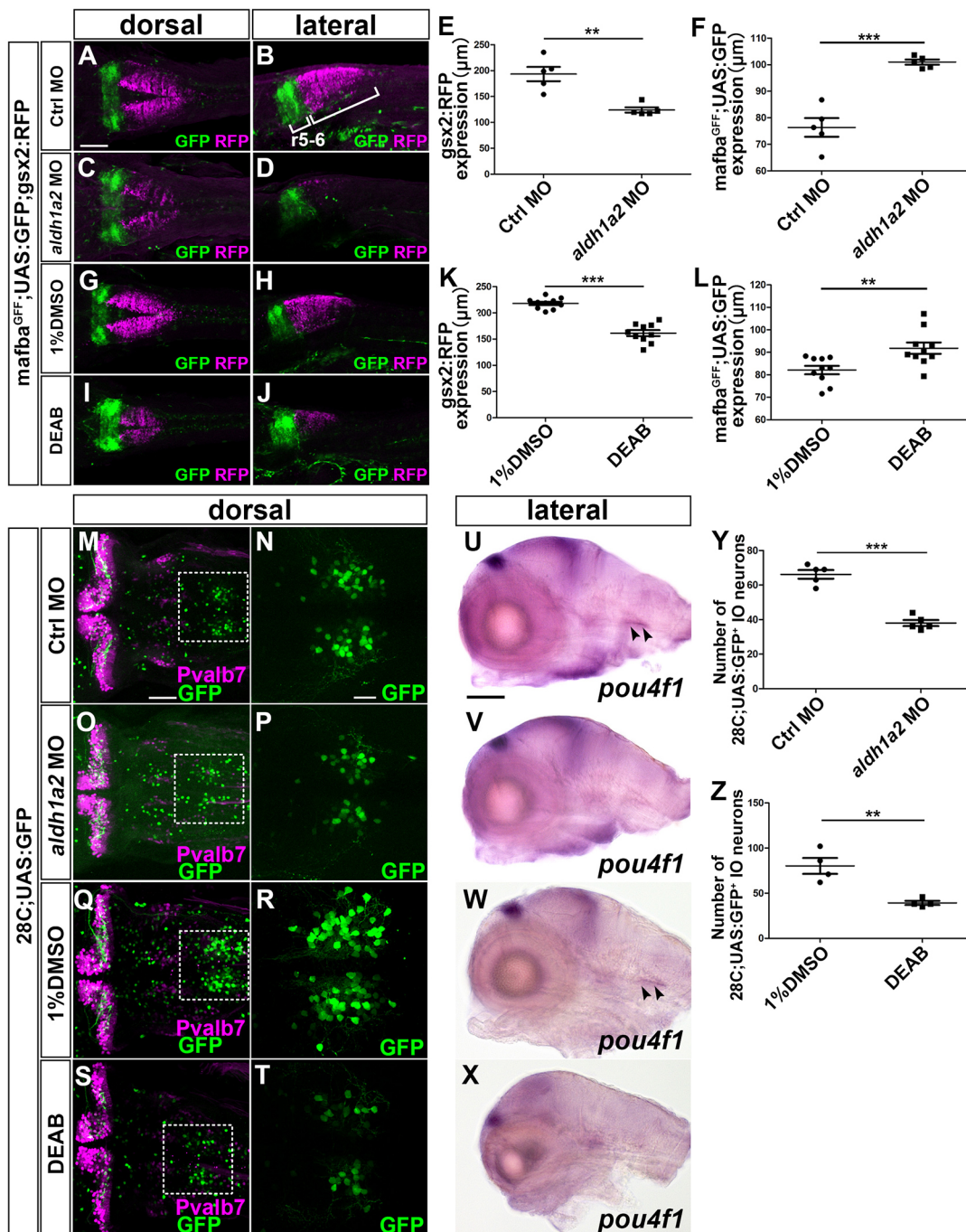
Fig. 9. RA signal positively controls *gsx2* expression and IO neuronal development. (A-D) 3 dpf control morphant (A,B, *n*=5) and *aldh1a2* morphant (C,D, *n*=5) mafba[GFF];UAS;GFP;gsx2:RFP larvae were stained using anti-RFP (magenta) and anti-GFP (green) antibodies. (E,F) Extent of gsx2:RFP (E) and mafbaGFF;UAS:GFP expression (F) in the hindbrain of the control and *aldh1a2* morphants. (G-J) mafba[GFF];UAS;GFP;gsx2:RFP larvae were treated with 1% DMSO (G,H, *n*=10) and 0.25 µM DEAB (I,J,H,I, *n*=10) from 6 to 22 hpf, fixed at 3 dpf, and stained using anti-GFP and anti-RFP antibodies. (K,L) Extent of gsx2: RFP (K) and mafba[GFF];UAS:GFP (L) expression in the hindbrain of larvae treated with DMSO or DEAB. (M-T) 5 dpf control morphant (M,N, *n*=5) and *aldh1a2* morphant (O,P, *n*=5), DMSO- (Q,R, *n*=4) or DEAB-treated (S,T, *n*=4) 28C;UAS:GFP larvae were stained using anti-Pvalb7 (magenta) and anti-GFP (green) antibodies. (N,P,R,T) Higher magnification of the boxes in M,O,Q,S. (U-X) Expression of *pou4f1* in 5 dpf control morphant (*n*=5), *aldh1a2* morphant (*n*=5), DMSO-treated (*n*=3) or DEAB-treated (*n*=3) larvae. (Y) The number of 28C;UAS:GFP^{+} IO neurons in 5 dpf control morphant and *aldh1a2* morphant larvae. (Z) Number of 28C;UAS:GFP^{+} IO neurons in 5 dpf larvae treated with DMSO and DEAB. **$P<0.01$; ***$P<0.001$ (Student's *t*-test). Data are mean±s.e.m. with individual values indicated. Scale bars: 100 µm in A (applies to A-D,G-J) and U (applies to U-X); 50 µm in M (applies to M,O,Q,S); 20 µm in N (applies to N,P,R,T).

Yamada et al., 2007). Although the mice and zebrafish phenotypes are slightly different, our data and those of others suggest that *ptf1a*-expressing progenitors give rise to PCs and IO neurons in both species, and also contribute to the development of DCN neurons in mice and of crest cells in zebrafish (Fig. 11).

A milder reduction of PCs in zebrafish suggest that other genes compensate for the lack of Ptf1a. In mice, bHLH-type proneural genes neurogenin 1 and 2 (*Neurog1* and *Neurog2*) and *Ascl1* are expressed in the ventricular zone of the dorsal hindbrain (Kim et al., 2008; Landsberg et al., 2005; Lundell et al., 2009; Zordan et al., 2008). In mice, *Neurog2*
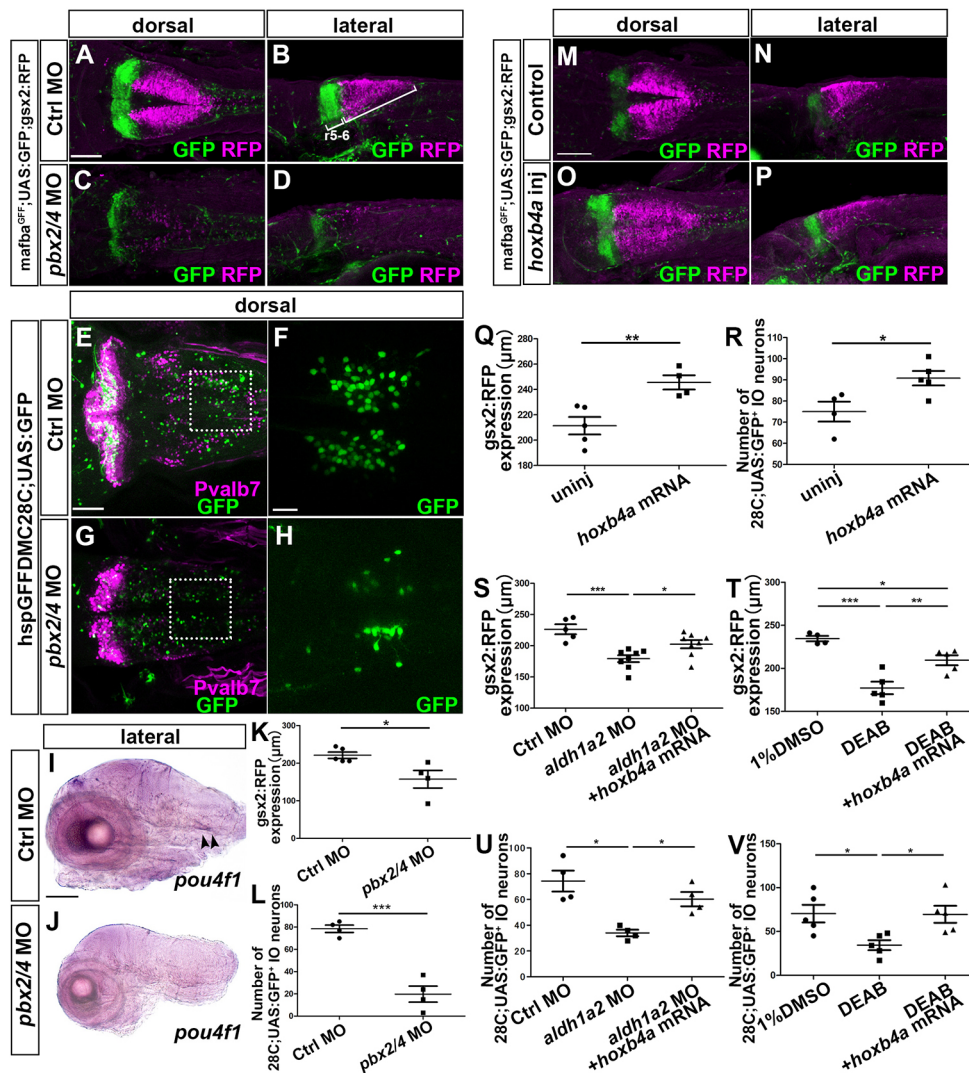
Fig. 10. Hox genes are involved in *gsx2* expression and IO neuronal development. (A-D) 3 dpf control morphant (A,B, *n*=5) and *pbx2/4* morphant (C,D, *n*=4) mafba^GFF;UAS;GFP;gsx2:RFP larvae were stained using anti-RFP (magenta) and anti-GFP (green) antibodies. (E-H) 5 dpf control morphant (E,F, *n*=4) and *pbx2/4* morphant (G,H, *n*=4) 28C;UAS:GFP larvae stained using anti-Pvalb7 (magenta) and anti-GFP (green) antibodies. (I,J) Expression of *pou4f1* in 5 dpf control morphant (I) and *pbx2/4* morphant (J) larvae. The *pou4f1* signal is marked by arrowheads. (K,L) Length of the gsx2:RFP⁺ hindbrain region (K) and number of 28C;UAS:GFP⁺ IO neurons (L) in control and *pbx2/4* morphant larvae. (M-P) 3 dpf control (M,N, *n*=4) and 25 pg *hoxb4a* RNA-injected (O,P, *n*=4) larvae were stained with anti-RFP (magenta) and anti-GFP (green) antibodies. (Q,R) Length of the gsx2:RFP⁺ hindbrain region (Q) and number of 28C;UAS:GFP⁺ neurons (R) in control and *hoxb4a* RNA-injected larvae. (S,T) Length of the gsx2:RFP⁺ hindbrain region in control (*n*=5), *aldh1a2* morphant (*n*=8) and *hoxb4a* RNA-injected *aldh1a2* morphant larvae (*n*=8) (S); in control (1% DMSO-treated, *n*=4), DEAB-treated (*n*=5), *hoxb4a* RNA-injected and DEAB-treated larvae (*n*=5) (T). (U,V) Number of 28C;UAS:GFP⁺ neurons in control (*n*=4), *aldh1a2* morphant (*n*=4), and *hoxb4a* RNA-injected *aldh1a2* morphant larvae (*n*=4) (U); in control (1% DMSO-treated, *n*=5), DEAB-treated (*n*=5), *hoxb4a* RNA-injected and DEAB-treated larvae (*n*=5) (V). *P<0.05; **P<0.01; ***P<0.001 (Student's *t*-test for K,L,Q,R, and one-way ANOVA with Tukey's multiple comparison test for S-V). Data are mean±s.e.m. with individual values indicated. Scale bars: 100 μm in A (applies to A-D), M (applies to M-P) and I (applies to I,J); 50 μm in E (applies to E,G); 20 μm in F (applies to F,H).

mutants show a reduction in number and defective dendritogenesis of PCs (Florio et al., 2012), while the *Ascl1* mutation leads to a reduction of cerebellar GABAergic interneurons and oligodendrocytes (Grimaldi et al., 2009; Sudarov et al., 2011), suggesting the involvement of other proneural genes in the development of PCs and other interneurons in the cerebellum. Zebrafish has *neurog1*, *ascl1a* and *ascl1b* but not *neurog2* (ZFIN, https://zfin.org). Some of these proneural genes may redundantly function with *ptf1a* in the development of PCs. Unlike PCs and crest cells, IO neurons were completely absent in *ptf1a* mutants (Fig. 3), indicating that Ptf1a is indispensable for IO neuronal development in both mice and zebrafish.

In addition to PCs, crest cells in MONs were reduced in *ptf1a* mutant larvae (Fig. S5). In mice, inhibitory neurons in DCNs are derived from *Ptf1a*-expressing neural progenitors in the r2-5 ventricular zone (Fujiyama et al., 2009). Although zebrafish do not have DCNs, there is a similarity between DCN and MON: they both receive input from hair cells (in the cochlear organ in mice or via the lateral line system in teleosts) (Yamamoto and Ito, 2005). The DCN and MON have a neural-circuit structure similar to the cerebellum and are thus called cerebellum-like structures (Bell et al., 2008; Oertel and Young, 2004). Although crest cells are excitatory, our data suggest that both crest cells and DCN inhibitory neurons are derived from *ptf1a*-expressing progenitors. It is tempting to speculate that the DCN and MON were derived from a common ancestral origin during evolution.
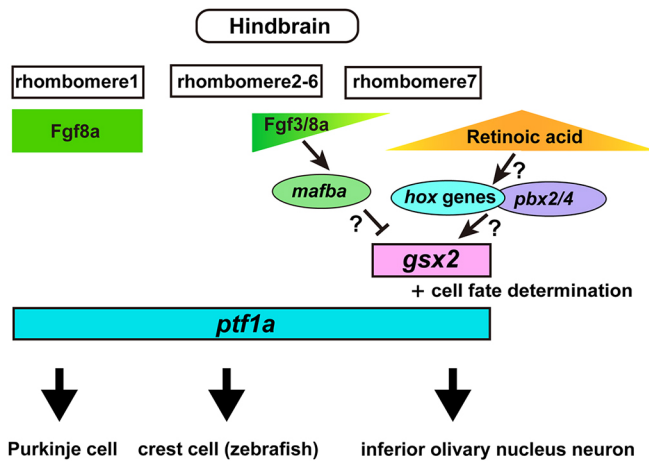
DEVELOPMENT

Fig. 11. Schematic diagram of the roles of Gsx2 in IO neuronal development.

Role of Gsx2 in the development of IO neurons

The *gsx2* mutants showed a strong reduction or loss of IO neurons (Fig. 2), indicating that Gsx2 is required for IO neuronal development. Previous studies in mice showed that *Gsx2* is expressed in the ventricular zone of the ventral telencephalon, hindbrain and spinal cord, and that it is required for the development of striatal neurons in the telencephalon, olfactory interneurons in the olfactory bulb and dorsal interneurons in the spinal cord (Corbin et al., 2000; Kriks et al., 2005; Szucsik et al., 1997). Therefore, although Gsx2 is involved in the development of different types of neurons, it plays a similar role in the specification of neurons from their progenitors in the ventricular zone of these brain regions.

In some *gsx2* mutants, a small number of IO neurons remained, and projected CFs to PCs (Fig. 2), suggesting the presence of genes that redundantly function with *gsx2* in IO progenitors. *gsx1*, which is a homologue of *gsx2*, is expressed in the hindbrain (r1-7) and spinal cord of zebrafish (Begemann et al., 2001). In mice, *Gsx1* and *Gsx2* redundantly function in LGE patterning and in the specification of dorsal interneurons of the spinal cord (Mizuguchi et al., 2006; Yun et al., 2003). Although the expression domains of *gsx1* and *gsx2* are different in the spinal cord of zebrafish (Satou et al., 2013), it is possible that *gsx1* is co-expressed with *gsx2* and cooperatively functions in the development of some IO neurons. A previous study showed the presence of IOs in the hindbrain of *Gsx2* mutant mice, although it is not clear whether IO neurons were reduced (Szucsik et al., 1997), suggesting that the IO phenotype of *Gsx2* mouse mutants are milder than in the phenotype of the *gsx2* zebrafish mutant. Expansion of *Gsx1* expression in *Gsx2* mutants was reported for the development of mouse LGE (Toresson and Campbell, 2001). Gsx1-mediated compensation of Gsx2 deficiency might function at lower levels in zebrafish than in mice. Future studies on *gsx1* expression and *gsx1* mutants will clarify this issue.

Different roles of Ptf1a and Gsx2 in IO neuronal development

The expression of *ptf1a* and *gsx2* in the caudal hindbrain was independent during early neurogenesis (Fig. 4). Whereas the *ptf1a* mutants showed an increase in apoptosis in the caudal hindbrain, the *gsx2* mutants did not (Fig. 5), suggesting different roles of *ptf1a* and *gsx2* in IO neuronal development. The phenotype of zebrafish *ptf1a* mutants is consistent with that of mouse *Ptf1a* mutants, which also showed increased apoptosis in the IO region (Yamada et al., 2007). These data imply that a major population of IO progenitors that did not differentiate to neurons died by apoptosis in the absence of *ptf1a*

in both mice and zebrafish. However, some cells derived from *Ptf1a*-expressing progenitors (*Ptf1a*-lineage cells) become precerebellar neurons that send mossy fibers in *Ptf1a* mutant mice (Yamada et al., 2007), suggesting a role of *Ptf1a* in fate determination of IO neurons in mice. However, in zebrafish, the *ptf1a/gsx2*-lineage cells (ptf1a: GFP+ and gsx2:RFP+ cells) were present in the dorsal hindbrain and did not migrate ventrally to where mossy fiber neurons are supposed to be located in *ptf1a* mutants (Figs S5 and S6). Therefore, even if some cells derived from IO progenitors undergo a change in fate, they are likely a small population in zebrafish.

In contrast to the *ptf1a* mutants, *gsx2*-lineage cells migrated ventrally from the ventricular zone and some of them differentiated to neurons that extended axons to the cerebellum region in *gsx2* mutants (Fig. S6). These neurons are potentially the nucleus commissure of Wallenberg. However, these fibers were also reduced in *gsx2* mutants (Fig. S6). In addition, mnx2b:GFF;UAS:GFP+ neurons located laterally to IOs were reduced in *gsx2* and *ptf1a* mutants (Figs 2 and 3). These data suggest that the development of these neurons depends on *gsx2*. We currently do not know what type(s) of neurons these *gsx2*-lineage cells were differentiated to in the absence of Gsx2. Nevertheless, our findings suggest that *ptf1a* is involved in neuronal differentiation, whereas *gsx2* is involved in the specification of IO neurons. Ptf1a and Gsx2 cooperatively control the development of IO neurons. Ascl1 and Gsx1/2 coordinately control the specification of dorsal glutamatergic sensory neurons in mice (Mizuguchi et al., 2006). Thus, cooperation between proneural gene(s) and *gsx*-family genes is a common mechanism that coordinately controls the differentiation and specification of a subset of neurons from their progenitors.

We further demonstrated that the co-expression of *ptf1a* and *gsx2* was not sufficient to induce IO neurons (Fig. 6). Other factors may function with Ptf1a and Gsx2 in IO neuronal development. One of the candidate co-factors is the bHLH-type transcription factor Olig3, which cooperates with Ptf1a in IO neuronal development in mice (Storm et al., 2009). Future studies will reveal a set of transcription factors that sufficiently initiates the genetic program of IO neuronal development.

gsx2 mediates Fgf and RA signals to specify IO neuronal fate

Inhibition of the signal of *fgf3* and *fgf8a*, which are known to be expressed in r4 and are involved in the specification of r5/6 (Maves et al., 2002; Walshe et al., 2002; Wiellette and Sive, 2004), led to reduced *mafba* expression, an expansion of *gsx2* expression, and an increase in the number of IO neurons (Fig. 7). The *mafba* mutants showed a slight increase in *gsx2* expression and in the number of IO neurons (Fig. 8). Fgf signal-mediated *mafba* expression has previously been reported for chicken (Marin and Charnay, 2000) and zebrafish (Ghosh et al., 2018). Collectively, these data indicate that the Fgf signal suppresses rostral expansion of *gsx2* expression in the caudal hindbrain and thereby limits the IO progenitor domain to r7; Mafba is at least partly involved in this regulation (Fig. 11). Fgf8a is involved in the formation of the cerebellum (Reifers et al., 1998). In *fgf3/fgf8a*-defective larvae, the number of IO neurons increased but PCs were absent (Fig. 7). Intriguingly, IO neurons project their axons rostrally to the optic tectum region even in the absence of PCs, which are the targets of CFs (Fig. 7), indicating the presence of a PC-independent axon guidance mechanism for CFs. Future studies will clarify this mechanism. As MafB directly activates *hoxb3* expression in mice (Manzanares et al., 1997), the *mafba-hoxb3* cascade may play a role in repressing *gsx2* expression and IO neuronal identity.

During early neurogenesis, *aldh1a2* is expressed in forming somites in mouse, chicken and zebrafish (Begemann et al., 2001;

Berggren et al., 1999; Blentic et al., 2003; Grandel et al., 2002; Niederreither et al., 1997). The treatment of mouse embryos with RA increased IO neurons (Yamamoto et al., 2005) but defective RA signals led to a reduced caudal hindbrain in zebrafish (Begemann et al., 2004, 2001; Grandel et al., 2002). We showed that the inhibition of RA signals resulted in reduced *gsx2* expression and IO neuronal development (Fig. 9). These data indicate that the RA signal positively controls *gsx2* expression and, subsequently, IO neuronal development. Hox genes function downstream of RA signals (reviewed by Nolte et al., 2019). Defects in the RA signal in zebrafish result in a strong reduction or absence of *hoxb4a* in the caudal hindbrain (Begemann et al., 2004, 2001; Grandel et al., 2002). *hoxb4a* enhancer-driven YFP expression was detected in IO neurons (Ma et al., 2009; Punnamoottil et al., 2008). *hoxb4* is a direct target of the RA receptor RAR/RXR complex in chickens (Gould et al., 1998). These data suggest that the RA signal controls caudal hindbrain identity through the expression of Hox genes, including *hoxb4a*, in the caudal hindbrain. As Hox paralogues function redundantly, it is difficult to address the roles of individual Hox genes. We demonstrated that the loss of Pbx2 and Pbx4, which function as co-factors for rostral Hox proteins harboring a YPWM motif (Johnson et al., 1995; Mann and Chan, 1996; Shanmugam et al., 1997), led to a strong reduction of *gsx2* expression and IO neurons (Fig. 10). Furthermore, misexpression of Hoxb4a, which harbors a YPWM motif, elicited the expansion of *gsx2* expression (Fig. 10). Expression of Hoxb4a at least partly rescued gsx2:RFP expression and 28C;UAS:GFP⁺ IO neurons in the *aldh1a2* morphant or in DEAB-treated larvae (Fig. 10). Our findings suggest that r7-expressed Hox genes, such as *hoxb4a*, function directly downstream of the RA signal to control *gsx2* expression and IO neuronal development. *pbx2/pbx4*-deficient larvae show defects in the function of most rostral Hox proteins and the loss of r2-6 identity (Waskiewicz et al., 2002). Although the number of PCs increased, the number of crest cells was normal in *pbx2/pbx4*-deficient larvae (Fig. 10), suggesting that the specification of PCs and crest cells does not rely on Pbx-interacting rostral Hox proteins. The RA-Hox cascade controls the specification of IO neurons from *ptf1a*-expressing progenitors by regulating *gsx2* expression (Fig. 11). Our study did not address whether MafBa and/or Hox proteins directly regulate *gsx2* expression in the caudal hindbrain. The zebrafish *gsx2* gene has an ∼800 bp element on the 3′ side of the open reading frame that displays partial sequence homology with the mouse *Gsx2* enhancer that can drive transgene expression in the mouse ventral telencephalon and caudal hindbrain (K.S., unpublished). Although the zebrafish element contains putative binding motifs of MafBa and Hox proteins, further analysis is required to understand the regulation of *gsx2* expression in the caudal hindbrain.

ptf1a-expressing neural progenitors give rise to three different neuron PCs, crest cells and IO neurons following positional signals. Gsx2 mediates Fgf and RA positional signals to specify IO neurons. Future studies will reveal genetic programs for the specification of PCs and crest cells. The identification of targets for Gsx2 and Ptf1a will clarify the mechanisms underlying the development and functionality of IO neurons.

MATERIALS AND METHODS
Zebrafish strain
The animal work in this study was approved by the Nagoya University Animal Experiment Committee and was conducted in accordance with the Regulations on Animal Experiments at Nagoya University. Wild-type zebrafish with the Oregon AB genetic background were used. For immunohistochemistry and whole-mount *in situ* hybridization, larvae were treated with 0.003% 1-phenyl-

2-thiourea (PTU) to inhibit the formation of pigmentation. *Tg(UAS:EGFP)* (nkuasgfp1aTg), *Tg(ptf1a:EGFP)*, *TgBAC(mnx2b:GFF)*, *TgBAC(gsx2: LOXP-Tomato-LOXP-GFP)* and *TgBAC(ptf1a:GAL4-VP16)* have been previously reported and characterized (Asakawa et al., 2013, 2008; Parsons et al., 2009; Pisharath et al., 2007; Satou et al., 2013). hspGFFDMC28C is a Gal4 trap line that drives UAS-dependent expression in IO neurons (Takeuchi et al., 2015). gSAIzGFFM35A is a *mafba* mutant in which the *mafba* exon is disrupted by the Gal4 gene trap, and is also known as *mafba*^*nkgsaizgffm35aGt*^ (Asakawa and Kawakami, 2018). The *Tg(UAS-hsp70l;gsx2BLRP-P2A-BirA-P2A-mCherry)* line, which harbors a transgene containing *gsx2*, biotin ligase recognition peptide (BLRP), 2A peptide sequences of porcine teschovirus-1 (P2A), biotin ligase (BirA) and mCherry genes, will be described elsewhere. The *mafba*^*b337*^ and *fgf8a*^*ti282a*^ mutants, known previously as *valentino* and *acerebellar*, respectively, have been described elsewhere (Moens et al., 1998; Reifers et al., 1998). The allele names of the *gsx2*^*Δ5*^, *gsx2*^*Δ8*^, *ptf1a*^*Δ4*^ and *ptf1a*^*+11*^ mutants established in this study are designated as *gsx2*^*nub32*^, *gsx2*^*nub33*^, *ptf1a*^*nub34*^ and *ptf1a*^*nub35*^, respectively, in ZFIN (https://zfin.org). The zebrafish were maintained at 28°C under a 14 h light and 10 h dark cycle. Embryos and larvae were maintained in embryonic medium (EM) (Westerfield, 2000).

Establishment of *gsx2* and *ptf1a* mutants by the CRISPR/Cas9 system
The gRNA targets were designed by the web software ZiFit Targeter 4.2 (http://zifit.partners.org/ZiFiT/) (Hwang et al., 2013; Mali et al., 2013). To generate gRNAs, the following oligonucleotides were used: 5′-TAGGCG-GAATTCCACTGCTCAA-3′ and 5′-AAACTTGAGCAGTGGAATTCC-G-3′ for *gsx2*^*Δ5*^; 5′-TAGGTCTTCCGGGACGGGCAGA-3′ and 5′-AAACTCTGCCCGTCCCGGAAG-3′ for *gsx2*^*Δ8*^; 5′-TAGGAAGAGGC-GGAGGCGCATG-3′ and 5′-AAACCATGCGCCTCCGCCTCTT-3′ for *ptf1a*^*Δ4*^; and 5′-TAGGCGTCAAGCTGCCAACGTC-3′ and 5′-AAACG-ACGTTGGCAGCTTGACG-3′ for *ptf1a*^*+11*^. gRNA and *Cas9* mRNA syntheses were performed as previously reported (Nimura et al., 2019). A solution containing 25 ng/μl gRNA and 100 ng/μl *Cas9* mRNA or 1000 ng/μl Cas9 protein (Toolgen) was injected into one-cell-stage embryos using a pneumatic microinjector (PV830, WPI). The insertion and/or deletion (indel) mutations on the target region were detected by a heteroduplex mobility assay (Ota et al., 2013). The mutations were confirmed by sequencing after subcloning the target regions amplified from the mutant genome into pTAC-2 (BioDynamics Laboratory).

Genotyping
To detect indel mutations, the following primers were used: 5′-GTGCGT-ATCCTCACACATCCACTCT-3′ and 5′-TGCCATCCTCTGGCAGAAC-G-3′ to detect the *gsx2*^*Δ5*^ mutation; 5′-CATTGGCATGCACTCTCCCG-3′ and 5′-TGAGGATACGCACAGCGGAC-3′ to detect the *gsx2*^*Δ8*^ mutation; 5′-ACCTCAGAGCTGTCCCCTCACAGA-3′ and 5′-GGCAGCTTGACG-CAACTGTT-3′ to detect the *ptf1a*^*Δ4*^ mutation; and 5′-GGAGGCGCAT-GAGGTCTGAAGT-3′ and 5′-GCAGTCCCTCGAAAGCATCG-3′ to detect the *ptf1a*^*+11*^ mutation. To identify gSAIzGFFM35A fish, 5′-CGAGGTAGGAGAAGGGCTGT-3′ and 5′-CTGGAGCGTTTGATGG-ATACAG-3′ primers were used to amplify about 200-bp PCR products from wild-type but not gSAIzGFFM35A genomic DNA. As *Tg(gsx2:loxp-DsRed-loxp-GFP)* are BAC Tg fish and contain a region of the *gsx2* exon1, we could not distinguish the wild-type allele of *gsx2* from the endogenous locus or the transgene in this fish with the primers described above. To detect wild-type and mutant alleles of *gsx2* in *gsx2*^*Δ5*^;*Tg(gsx2: LOXP-To-mato-LOXP-GFP)* fish, the following primers were used: 5′-CCATCAG-CATCTCGCTCAG-3′ and 5′-CAGTGTGAAGCCTTGTCCCTCG-3′. After PCR amplification, PCR products were digested with *Xho*I. The wild-type *gsx2* allele gave rise to two bands, 21 and 257 bp fragments, while the mutant allele displayed a single band as it cannot be digested with *Xho*I. To detect the *fgf8a*^*ti282a*^ mutation, 5′-CAGGAGGGGGAAACTGATTGTCT-AG-3′ and 5′-CCCTTTCTAGGTGGGATTCTTCTC-3′ primers were used. After PCR amplification, PCR products were digested with XbaI. The wild-type PCR products could not be digested, whereas the mutant PCR products gave rise to 130 and 20 bp DNA fragments.

Injection of antisense morpholino oligonucleotides

fgf3, *aldh1a2*, *pbx2* and *pbx4* MOs were translation-blocking antisense MOs that were previously reported (Begemann et al., 2001; Maves et al., 2007; Wiellette and Sive, 2004). 0.3 mM *fgf3* MO, 0.1 mM *aldh1a2* MO, 0.03 mM *pbx2* MO2, 0.06 mM *pbx2* MO3, 0.06 mM *pbx4* MO1 or 0.06 mM *pbx4* MO2 (1 nl) were injected into one-cell-stage embryos. As a control, we used a standard control MO: 5′-CCTCTTACCTCAGTTACAATTTATA-3′. These MOs were obtained from Gene Tool.

Treatment with chemical inhibitors

DEAB (Wako) and SU5402 (Calbiochem) were dissolved in DMSO at 100 mM and 20 mM, respectively. Embryos were treated with 0.25 µM DEAB or 1.0, 2.5, 5.0 and 200 µM SU5402 in 0.003% PTU/EM from 6 to 22 h post fertilization (hpf).

cDNA cloning

Total RNA was isolated from 5 or 12 dpf zebrafish larvae using TRI Reagent (Molecular Research Center). cDNA was generated using ReverTra Ace (Toyobo). DNA fragments for *gsx2* or *foxp2* were amplified from the 5-dpf cDNA library using the primers 5′-GACTCTTTGATTATCAAGGATCC-CG-3′ (F) and 5′-CGTCTTCTGAGCGCGGATAAT-3′ (R) for *gsx2*, and 5′-CCATGGAGGATAATGGGATG-3′ (F) and 5′-TGAGGTAAATTTG-GGGGTGA-3′ (R) for *foxp2*, and subcloned to pGEMT-easy (Promega) and pTA2 (Toyobo), respectively (pGEMTe-*gsx2* and pTA2-*foxp2*). Three DNA fragments for *grm5a* (*grm5a*-A, *grm5a*-B and *grm5a*-C) were amplified from zebrafish genomic DNA with the primers 5′-CACTTTTC-TCCGTCCACCAT-3′ (F) and 5′-GCGATCTGGGGAATATTGAA-3′ (R) for *grm5a*-A, 5′-ACCTTCAGTGGGGAGATCCT-3′ (F) and 5′-GATGA-AGAGTGCCACGATGA-3′ (R) for *grm5a*-B, and 5′-CGGCCATTATC-AAACCATTC-3′ (F) and 5′-TGACGGTAGGATGGTGAACA-3′ (R) for *grm5a*-C, and subcloned into pTAC2 (pTAC2-*grm5a*-A/B/C). Three DNA fragments for *pou4f1* (*pou4f1*-A, *pou4f1*-B and *pou4f1*-C) were amplified from zebrafish genomic DNA with the primers 5′- GCGATGAGCTGAG-ATGAGAG-3′ (F) and 5′-AGCTCGAGTGCAGAGTTGTG-3′ (R) for *pou4f1*-A, 5′-GGGTAAGAGTCACCCGTTCA-3′ (F) and 5′-AGTCCGT-TGTTGACGAGTCC-3′ (R) for *pou4f1*-B, and 5′- CAATTAACGACTC-GGACACG-3′ (F) and 5′-TCAGCTATAGCCGCGATTTT-3′ for *pou4f1*-C, and subcloned to pTAC2 (pTAC2-*pou4f1*-A/B/C). The full-length cDNA for *hoxb4a* was amplified from the 12 hpf cDNA library with the following primers: 5′-GGAATTCATGGCCATGAGTTCCTATTT-3′ (F) and 5′-GCTCTAGACTATAGACTTGGCGGAGGTCC-3′ (R). The DNA fragment was digested with EcoRI and XbaI, and subcloned into pCS2+MT (pCS2+MT-*hoxb4a*).

In situ hybridization

Whole mount *in situ* hybridization was performed as previously reported (Bae et al., 2009). Detection of *ptf1a* and *pou4f1* riboprobes has been described previously (Bae et al., 2009; Kani et al., 2010). A digoxigenin (DIG)-labeled riboprobe was made from pTAC2 -*grm5a*-A/B/C, pTA2-*foxp2*, pGEMTe-*gsx2* and pTAC2-*pou4f1*-A/B/C, using SP6, T3 or T7 RNA polymerase after digestion with restriction enzymes. For *grm5a* and *pou4f1*, a mixture of three riboprobes was used (*grm5a* in Figs 2 and 3; *pou4f1* in Fig. S3). To detect transcripts in the IO neurons of 5 dpf larvae, the head regions rostral to the spinal cord of larvae were cut and used for *in situ* hybridization. To stain larval heads, they were hybridized overnight at 65°C for 72 h and incubated overnight with 1/2000 alkaline-phosphatase conjugated with anti-DIG Fab fragment (Roche) at 4°C for 3 nights. BM-purple signals were acquired using an AxioPlan-2 microscope equipped with an AxioCam CCD camera (Zeiss).

Immunohistochemistry and counting IO neurons

For immunohistochemistry, anti-parvalbumin7 (1/1000, mouse monoclonal, ascites) (Bae et al., 2009), anti-GFP (1/1000, rat, Nacalai Tesque, Cat# 04404-84), anti-DsRed (1/1000, rabbit, Clontech Laboratories, 632496) and anti-cleaved caspase 3 (1/500, rabbit, Cell Signaling Technology, 9661) were used. Alexa Fluor 488 goat anti-rat IgG (H+L, Thermo Fisher Scientific, A-11006), CF488A goat anti-rat IgG (H+L, Biotium, 20023), CF488A goat anti-mouse

IgG (H+L, Biotium, 20018-1), CF568 goat anti-mouse IgG (H+L, Biotium, 20301-1) and CF568 goat anti-rabbit IgG (H+L, Biotium, 20103) were used as the secondary antibodies. Larvae were immunostained as described previously (Bae et al., 2009). Some fixed samples were optically cleared with SeeDB reagent as previously reported (Ke et al., 2013; Ke and Imai, 2014). An LSM700 confocal laser-scanning microscope was used to obtain fluorescence images. To count IO neurons, confocal optical sections of the ventral region of the caudal hindbrain (120 µm×120 µm×52 µm) were obtained from immunostained hspGFFDMC28C;*Tg(5xUAS:EGFP)* larvae. As 28C;UAS:GFP⁺ cells that were located in this region extended their axons rostrally, they were considered as IO neurons and the number of GFP⁺ cells were counted manually.

mRNA injection

To make *hoxb4a* mRNA for expression, pCS2+MT-*hoxb4a* was linearized with NotI and transcribed with SP6 RNA polymerase in the presence of a $G(5′)ppp(5′)G$ RNA cap structure analog (New England BioLabs). One-cell-stage embryos were injected with 25 pg of *hoxb4a* mRNA.

Statistics

Data were analyzed for statistical significance using Student's *t*-test, Welch's *t*-test and one-way ANOVA using Graphpad PRISM (ver. 5.1).

Supplementary information
Supplementary information available online at
https://dev.biologists.org/lookup/doi/10.1242/dev.190603.supplemental

Peer review history
The peer review history is available online at
https://dev.biologists.org/lookup/doi/10.1242/dev.190603.reviewer-comments.pdf

References
Akitake, C. M., Macurak, M., Halpern, M. E. and Goll, M. G. (2011). Transgenerational analysis of transcriptional silencing in zebrafish. *Dev. Biol.* **352**, 191-201. doi:10.1016/j.ydbio.2011.01.002

Ambrosiani, J., Armengol, J. A., Martinez, S. and Puelles, L. (1996). The avian inferior olive derives from the alar neuroepithelium of the rhombomeres 7 and 8: an analysis by using chick-quail chimeric embryos. *Neuroreport* **7**, 1285-1288. doi:10.1097/00001756-199605170-00013

Asakawa, K. and Kawakami, K. (2018). Protocadherin-mediated cell repulsion controls the central topography and efferent projections of the abducens nucleus. *Cell Rep.* **24**, 1562-1572. doi:10.1016/j.celrep.2018.07.024

Asakawa, K., Suster, M. L., Mizusawa, K., Nagayoshi, S., Kotani, T., Urasaki, A., Kishimoto, Y., Hibi, M. and Kawakami, K. (2008). Genetic dissection of neural

circuits by *Tol2* transposon-mediated Gal4 gene and enhancer trapping in zebrafish. *Proc. Natl. Acad. Sci. USA* **105**, 1255-1260. doi:10.1073/pnas. 0704963105

Asakawa, K., Abe, G. and Kawakami, K. (2013). Cellular dissection of the spinal cord motor column by BAC transgenesis and gene trapping in zebrafish. *Front. Neural Circuits* **7**, 100. doi:10.3389/fncir.2013.00100

Bae, Y.-K., Kani, S., Shimizu, T., Tanabe, K., Nojima, H., Kimura, Y., Higashijima, S. and Hibi, M. (2009). Anatomy of zebrafish cerebellum and screen for mutations affecting its development. *Dev. Biol.* **330**, 406-426. doi:10. 1016/j.ydbio.2009.04.013

Begemann, G., Schilling, T. F., Rauch, G. J., Geisler, R. and Ingham, P. W. (2001). The zebrafish *neckless* mutation reveals a requirement for *raldh2* in mesodermal signals that pattern the hindbrain. *Development* **128**, 3081-3094.

Begemann, G., Marx, M., Mebus, K., Meyer, A. and Bastmeyer, M. (2004). Beyond the *neckless* phenotype: influence of reduced retinoic acid signaling on motor neuron development in the zebrafish hindbrain. *Dev. Biol.* **271**, 119-129. doi:10.1016/j.ydbio.2004.03.033

Bell, C. C., Han, V. and Sawtell, N. B. (2008). Cerebellum-like structures and their implications for cerebellar function. *Annu. Rev. Neurosci.* **31**, 1-24. doi:10.1146/ annurev.neuro.30.051606.094225

Berggren, K., McCaffery, P., Dräger, U. and Forehand, C. J. (1999). Differential distribution of retinoic acid synthesis in the chicken embryo as determined by immunolocalization of the retinoic acid synthetic enzyme, RALDH-2. *Dev. Biol.* **210**, 288-304. doi:10.1006/dbio.1999.9286

Blentic, A., Gale, E. and Maden, M. (2003). Retinoic acid signalling centres in the avian embryo identified by sites of expression of synthesising and catabolising enzymes. *Dev. Dyn.* **227**, 114-127. doi:10.1002/dvdy.10292

Cambronero, F. and Puelles, L. (2000). Rostrocaudal nuclear relationships in the avian medulla oblongata: a fate map with quail chick chimeras. *J. Comp. Neurol.* **427**, 522-545. doi:10.1002/1096-9861(20001127)427:4<522::AID-CNE3>3.0. CO;2-Y

Corbin, J. G., Gaiano, N., Machold, R. P., Langston, A. and Fishell, G. (2000). The *Gsh2* homeodomain gene controls multiple aspects of telencephalic development. *Development* **127**, 5007-5020.

Dupé, V. and Lumsden, A. (2001). Hindbrain patterning involves graded responses to retinoic acid signalling. *Development* **128**, 2199-2208.

Ferland, R. J., Cherry, T. J., Preware, P. O., Morrisey, E. E. and Walsh, C. A. (2003). Characterization of Foxp2 and Foxp1 mRNA and protein in the developing and mature brain. *J. Comp. Neurol.* **460**, 266-279. doi:10.1002/cne.10654

Florio, M., Leto, K., Muzio, L., Tinterri, A., Badaloni, A., Croci, L., Zordan, P., Barili, V., Albieri, I., Guillemot, F. et al. (2012). Neurogenin 2 regulates progenitor cell-cycle progression and Purkinje cell dendritogenesis in cerebellar development. *Development* **139**, 2308-2320. doi:10.1242/dev.075861

Fujita, H. and Sugihara, I. (2012). FoxP2 expression in the cerebellum and inferior olive: development of the transverse stripe-shaped expression pattern in the mouse cerebellar cortex. *J. Comp. Neurol.* **520**, 656-677. doi:10.1002/cne.22760

Fujiyama, T., Yamada, M., Terao, M., Terashima, T., Hioki, H., Inoue, Y. U., Inoue, T., Masuyama, N., Obata, K., Yanagawa, Y. et al. (2009). Inhibitory and excitatory subtypes of cochlear nucleus neurons are defined by distinct bHLH transcription factors, Ptf1a and Atoh1. *Development* **136**, 2049-2058. doi:10. 1242/dev.033480

Gavalas, A. and Krumlauf, R. (2000). Retinoid signalling and hindbrain patterning. *Curr. Opin. Genet. Dev.* **10**, 380-386. doi:10.1016/S0959-437X(00)00100-3

Ghosh, P., Maurer, J. M. and Sagerström, C. G. (2018). Analysis of novel caudal hindbrain genes reveals different regulatory logic for gene expression in rhombomere 4 versus 5/6 in embryonic zebrafish. *Neural Dev.* **13**, 13. doi:10. 1186/s13064-018-0112-y

Gould, A., Itasaki, N. and Krumlauf, R. (1998). Initiation of rhombomeric *Hoxb4* expression requires induction by somites and a retinoid pathway. *Neuron* **21**, 39-51. doi:10.1016/S0896-6273(00)80513-9

Grandel, H., Lun, K., Rauch, G. J., Rhinn, M., Piotrowski, T., Houart, C., Sordino, P., Küchler, A. M., Schulte-Merker, S., Geisler, R. et al. (2002). Retinoic acid signalling in the zebrafish embryo is necessary during pre-segmentation stages to pattern the anterior-posterior axis of the CNS and to induce a pectoral fin bud. *Development* **129**, 2851-2865.

Grimaldi, P., Parras, C., Guillemot, F., Rossi, F. and Wassef, M. (2009). Origins and control of the differentiation of inhibitory interneurons and glia in the cerebellum. *Dev. Biol.* **328**, 422-433. doi:10.1016/j.ydbio.2009.02.008

Hashimoto, M. and Hibi, M. (2012). Development and evolution of cerebellar neural circuits. *Dev. Growth Differ.* **54**, 373-389. doi:10.1111/j.1440-169X.2012.01348.x

Haug, M. F., Gesemann, M., Mueller, T. and Neuhauss, S. C. F. (2013). Phylogeny and expression divergence of metabotropic glutamate receptor genes in the brain of zebrafish (*Danio rerio*). *J. Comp. Neurol.* **521**, 1533-1560. doi:10.1002/cne. 23240

Hibi, M. and Shimizu, T. (2012). Development of the cerebellum and cerebellar neural circuits. *Dev. Neurobiol.* **72**, 282-301. doi:10.1002/dneu.20875

Hoshino, M. (2012). Neuronal subtype specification in the cerebellum and dorsal hindbrain. *Dev. Growth Differ.* **54**, 317-326. doi:10.1111/j.1440-169X.2012. 01330.x

Hoshino, M., Nakamura, S., Mori, K., Kawauchi, T., Terao, M., Nishimura, Y. V., Fukuda, A., Fuse, T., Matsuo, N., Sone, M. et al. (2005). Ptf1a, a bHLH transcriptional gene, defines GABAergic neuronal fates in cerebellum. *Neuron* **47**, 201-213. doi:10.1016/j.neuron.2005.06.007

Hsieh-Li, H. M., Witte, D. P., Szucsik, J. C., Weinstein, M., Li, H. and Potter, S. S. (1995). *Gsh-2*, a murine homeobox gene expressed in the developing brain. *Mech. Dev.* **50**, 177-186. doi:10.1016/0925-4773(94)00334-J

Hwang, W. Y., Fu, Y., Reyon, D., Maeder, M. L., Tsai, S. Q., Sander, J. D., Peterson, R. T., Yeh, J.-R. J. and Joung, J. K. (2013). Efficient genome editing in zebrafish using a CRISPR-Cas system. *Nat. Biotechnol.* **31**, 227-229. doi:10. 1038/nbt.2501

Johnson, F. B., Parker, E. and Krasnow, M. A. (1995). Extradenticle protein is a selective cofactor for the *Drosophila* homeotics: role of the homeodomain and YPWM amino acid motif in the interaction. *Proc. Natl. Acad. Sci. U S A* **92**, 739-743. doi:10.1073/pnas.92.3.739

Kani, S., Bae, Y.-K., Shimizu, T., Tanabe, K., Satou, C., Parsons, M. J., Scott, E., Higashijima, S.-I. and Hibi, M. (2010). Proneural gene-linked neurogenesis in zebrafish cerebellum. *Dev. Biol.* **343**, 1-17. doi:10.1016/j.ydbio.2010.03.024

Kawauchi, D., Taniguchi, H., Watanabe, H., Saito, T. and Murakami, F. (2006). Direct visualization of nucleogenesis by precerebellar neurons: involvement of ventricle-directed, radial fibre-associated migration. *Development* **133**, 1113-1123. doi:10.1242/dev.02283

Ke, M.-T. and Imai, T. (2014). Optical clearing of fixed brain samples using SeeDB. *Curr. Protoc. Neurosci.* **66**, 2.22.21-22.22.19. doi:10.1002/0471142301. ns0222s66

Ke, M.-T., Fujimoto, S. and Imai, T. (2013). SeeDB: a simple and morphology-preserving optical clearing agent for neuronal circuit reconstruction. *Nat. Neurosci.* **16**, 1154-1161. doi:10.1038/nn.3447

Kim, E. J., Battiste, J., Nakagawa, Y. and Johnson, J. E. (2008). Ascl1 (Mash1) lineage cells contribute to discrete cell populations in CNS architecture. *Mol. Cell. Neurosci.* **38**, 595-606. doi:10.1016/j.mcn.2008.05.008

Kriks, S., Lanuza, G. M., Mizuguchi, R., Nakafuku, M. and Goulding, M. (2005). Gsh2 is required for the repression of Ngn1 and specification of dorsal interneuron fate in the spinal cord. *Development* **132**, 2991-3002. doi:10.1242/dev.01878

Landsberg, R. L., Awatramani, R. B., Hunter, N. L., Farago, A. F., DiPietrantonio, H. J., Rodriguez, C. I. and Dymecki, S. M. (2005). Hindbrain rhombic lip is comprised of discrete progenitor cell populations allocated by Pax6. *Neuron* **48**, 933-947. doi:10.1016/j.neuron.2005.11.031

Lundell, T. G., Zhou, Q. and Doughty, M. L. (2009). Neurogenin1 expression in cell lineages of the cerebellar cortex in embryonic and postnatal mice. *Dev. Dyn.* **238**, 3310-3325. doi:10.1002/dvdy.22165

Ma, L.-H., Punnamoottil, B., Rinkwitz, S. and Baker, R. (2009). Mosaic *hoxb4a* neuronal pleiotropism in zebrafish caudal hindbrain. *PLoS ONE* **4**, e5944. doi:10. 1371/journal.pone.0005944

Mali, P., Yang, L., Esvelt, K. M., Aach, J., Guell, M., DiCarlo, J. E., Norville, J. E. and Church, G. M. (2013). RNA-guided human genome engineering via Cas9. *Science* **339**, 823-826. doi:10.1126/science.1232033

Mann, R. S. and Chan, S.-K. (1996). Extra specificity from *extradenticle*: the partnership between HOX and PBX/EXD homeodomain proteins. *Trends Genet.* **12**, 258-262. doi:10.1016/0168-9525(96)10026-3

Manzanares, M., Cordes, S., Kwan, C.-T., Sham, M. H., Barsh, G. S. and Krumlauf, R. (1997). Segmental regulation of *Hoxb*-3 by *kreisler*. *Nature* **387**, 191-195. doi:10.1038/387191a0

Marin, F. and Charnay, P. (2000). Hindbrain patterning: FGFs regulate *Krox20* and *mafB/kr* expression in the otic/preotic region. *Development* **127**, 4925-4935.

Maves, L. and Kimmel, C. B. (2005). Dynamic and sequential patterning of the zebrafish posterior hindbrain by retinoic acid. *Dev. Biol.* **285**, 593-605. doi:10. 1016/j.ydbio.2005.07.015

Maves, L., Jackman, W. and Kimmel, C. B. (2002). FGF3 and FGF8 mediate a rhombomere 4 signaling activity in the zebrafish hindbrain. *Development* **129**, 3825-3837.

Maves, L., Waskiewicz, A. J., Paul, B., Cao, Y., Tyler, A., Moens, C. B. and Tapscott, S. J. (2007). Pbx homeodomain proteins direct Myod activity to promote fast-muscle differentiation. *Development* **134**, 3371-3382. doi:10.1242/ dev.003905

Maves, L., Tyler, A., Moens, C. B. and Tapscott, S. J. (2009). Pbx acts with Hand2 in early myocardial differentiation. *Dev. Biol.* **333**, 409-418. doi:10.1016/j.ydbio. 2009.07.004

Mizuguchi, R., Kriks, S., Cordes, R., Gossler, A., Ma, Q. and Goulding, M. (2006). *Ascl1* and *Gsh1/2* control inhibitory and excitatory cell fate in spinal sensory interneurons. *Nat. Neurosci.* **9**, 770-778. doi:10.1038/nn1706

Moens, C. B., Cordes, S. P., Giorgianni, M. W., Barsh, G. S. and Kimmel, C. B. (1998). Equivalence in the genetic control of hindbrain segmentation in fish and mouse. *Development* **125**, 381-391.

Mohammadi, M., McMahon, G., Sun, L., Tang, C., Hirth, P., Yeh, B. K., Hubbard, S. R. and Schlessinger, J. (1997). Structures of the tyrosine kinase domain of fibroblast growth factor receptor in complex with inhibitors. *Science* **276**, 955-960. doi:10.1126/science.276.5314.955

Niederreither, K., McCaffery, P., Dräger, U. C., Chambon, P. and Dollé, P. (1997). Restricted expression and retinoic acid-induced downregulation of the

retinaldehyde dehydrogenase type 2 (RALDH-2) gene during mouse development. *Mech. Dev.* **62**, 67-78. doi:10.1016/S0925-4773(96)00653-3

Niederreither, K., Vermot, J., Schuhbaur, B., Chambon, P. and Dollé, P. (2000). Retinoic acid synthesis and hindbrain patterning in the mouse embryo. *Development* **127**, 75-85.

Nimura, T., Itoh, T., Hagio, H., Hayashi, T., Di Donato, V., Takeuchi, M., Itoh, T., Inoguchi, F., Sato, Y., Yamamoto, N. et al. (2019). Role of Reelin in cell positioning in the cerebellum and the cerebellum-like structure in zebrafish. *Dev. Biol.* **455**, 393-408. doi:10.1016/j.ydbio.2019.07.010

Nolte, C., De Kumar, B. and Krumlauf, R. (2019). *Hox* genes: Downstream "effectors" of retinoic acid signaling in vertebrate embryogenesis. *Genesis* **57**, e23306. doi:10.1002/dvg.23306

Oertel, D. and Young, E. D. (2004). What's a cerebellar circuit doing in the auditory system? *Trends Neurosci.* **27**, 104-110. doi:10.1016/j.tins.2003.12.001

Ota, S., Hisano, Y., Muraki, M., Hoshijima, K., Dahlem, T. J., Grunwald, D. J., Okada, Y. and Kawahara, A. (2013). Efficient identification of TALEN-mediated genome modifications using heteroduplex mobility assays. *Genes Cells* **18**, 450-458. doi:10.1111/gtc.12050

Parsons, M. J., Pisharath, H., Yusuff, S., Moore, J. C., Siekmann, A. F., Lawson, N. and Leach, S. D. (2009). Notch-responsive cells initiate the secondary transition in larval zebrafish pancreas. *Mech. Dev.* **126**, 898-912. doi:10.1016/j.mod.2009.07.002

Pisharath, H., Rhee, J. M., Swanson, M. A., Leach, S. D. and Parsons, M. J. (2007). Targeted ablation of beta cells in the embryonic zebrafish pancreas using *E. coli* nitroreductase. *Mech. Dev.* **124**, 218-229. doi:10.1016/j.mod.2006.11.005

Punnamoottil, B., Kikuta, H., Pezeron, G., Erceg, J., Becker, T. S. and Rinkwitz, S. (2008). Enhancer detection in zebrafish permits the identification of neuronal subtypes that express Hox4 paralogs. *Dev. Dyn.* **237**, 2195-2208. doi:10.1002/dvdy.21618

Reifers, F., Böhli, H., Walsh, E. C., Crossley, P. H., Stainier, D. Y. and Brand, M. (1998). *Fgf8* is mutated in zebrafish *acerebellar* (*ace*) mutants and is required for maintenance of midbrain-hindbrain boundary development and somitogenesis. *Development* **125**, 2381-2395.

Russo, J. E. (1997). Inhibition of mouse and human class 1 aldehyde dehydrogenase by 4-(N,N-dialkylamino)benzaldehyde compounds. *Adv. Exp. Med. Biol.* **414**, 217-224. doi:10.1007/978-1-4615-5871-2_25

Satou, C., Kimura, Y., Hirata, H., Suster, M. L., Kawakami, K. and Higashijima, S.-I. (2013). Transgenic tools to characterize neuronal properties of discrete populations of zebrafish neurons. *Development* **140**, 3927-3931. doi:10.1242/dev.099531

Shanmugam, K., Featherstone, M. S. and Saragovi, H. U. (1997). Residues flanking the HOX YPWM motif contribute to cooperative interactions with PBX. *J. Biol. Chem.* **272**, 19081-19087. doi:10.1074/jbc.272.30.19081

Shimizu, T., Bae, Y.-K. and Hibi, M. (2006). Cdx-Hox code controls competence for responding to Fgfs and retinoic acid in zebrafish neural tissue. *Development* **133**, 4709-4719. doi:10.1242/dev.02660

Storm, R., Cholewa-Waclaw, J., Reuter, K., Bröhl, D., Sieber, M., Treier, M., Müller, T. and Birchmeier, C. (2009). The bHLH transcription factor Olig3 marks the dorsal neuroepithelium of the hindbrain and is essential for the development of brainstem nuclei. *Development* **136**, 295-305. doi:10.1242/dev.027193

Sudarov, A., Turnbull, R. K., Kim, E. J., Lebel-Potter, M., Guillemot, F. and Joyner, A. L. (2011). *Ascl1* genetics reveals insights into cerebellum local circuit assembly. *J. Neurosci.* **31**, 11055-11069. doi:10.1523/JNEUROSCI.0479-11.2011

Szucsik, J. C., Witte, D. P., Li, H., Pixley, S. K., Small, K. M. and Potter, S. S. (1997). Altered forebrain and hindbrain development in mice mutant for the *Gsh*-2 homeobox gene. *Dev. Biol.* **191**, 230-242. doi:10.1006/dbio.1997.8733

Takeuchi, M., Matsuda, K., Yamaguchi, S., Asakawa, K., Miyasaka, N., Lal, P., Yoshihara, Y., Koga, A., Kawakami, K., Shimizu, T. et al. (2015). Establishment of Gal4 transgenic zebrafish lines for analysis of development of cerebellar neural circuitry. *Dev. Biol.* **397**, 1-17. doi:10.1016/j.ydbio.2014.09.030

Tambalo, M., Mitter, R. and Wilkinson, D. G. (2020). A single cell transcriptome atlas of the developing zebrafish hindbrain. *Development* **147**, dev184143. doi:10.1242/dev.184143

Toresson, H. and Campbell, K. (2001). A role for *Gsh1* in the developing striatum and olfactory bulb of *Gsh2* mutant mice. *Development* **128**, 4769-4780.

Waclaw, R. R., Wang, B., Pei, Z., Ehrman, L. A. and Campbell, K. (2009). Distinct temporal requirements for the homeobox gene *Gsx2* in specifying striatal and olfactory bulb neuronal fates. *Neuron* **63**, 451-465. doi:10.1016/j.neuron.2009.07.015

Walshe, J., Maroon, H., McGonnell, I. M., Dickson, C. and Mason, I. (2002). Establishment of hindbrain segmental identity requires signaling by FGF3 and FGF8. *Curr. Biol.* **12**, 1117-1123. doi:10.1016/S0960-9822(02)00899-0

Waskiewicz, A. J., Rikhof, H. A. and Moens, C. B. (2002). Eliminating zebrafish pbx proteins reveals a hindbrain ground state. *Dev. Cell* **3**, 723-733. doi:10.1016/S1534-5807(02)00319-2

Westerfield, M. (2000). The Zebrafish Book: A Guide for the Laboratory Use of Zebrafish, 4th edn, University of Oregon Press. https://zfin.org/zf_info/zfbook/zfbk.html

Wiellette, E. L. and Sive, H. (2004). Early requirement for *fgf8* function during hindbrain pattern formation in zebrafish. *Dev. Dyn.* **229**, 393-399. doi:10.1002/dvdy.10464

Xue, H.-G., Yamamoto, N., Yang, C.-Y., Imura, K. and Ito, H. (2004). Afferent connections of the corpus cerebelli in holocentrid teleosts. *Brain Behav. Evol.* **64**, 242-258. doi:10.1159/000080244

Yamada, M., Terao, M., Terashima, T., Fujiyama, T., Kawaguchi, Y., Nabeshima, Y.-I. and Hoshino, M. (2007). Origin of climbing fiber neurons and their developmental dependence on *Ptf1a*. *J. Neurosci.* **27**, 10924-10934. doi:10.1523/JNEUROSCI.1423-07.2007

Yamamoto, N. and Ito, H. (2005). Fiber connections of the central nucleus of semicircular torus in cyprinids. *J. Comp. Neurol.* **491**, 186-211. doi:10.1002/cne.20683

Yamamoto, M., Fujinuma, M., Hirano, S., Hayakawa, Y., Clagett-Dame, M., Zhang, J. and McCaffery, P. (2005). Retinoic acid influences the development of the inferior olivary nucleus in the rodent. *Dev. Biol.* **280**, 421-433. doi:10.1016/j.ydbio.2005.02.007

Yun, K., Garel, S., Fischman, S. and Rubenstein, J. L. R. (2003). Patterning of the lateral ganglionic eminence by the *Gsh1* and *Gsh2* homeobox genes regulates striatal and olfactory bulb histogenesis and the growth of axons through the basal ganglia. *J. Comp. Neurol.* **461**, 151-165. doi:10.1002/cne.10685

Zordan, P., Croci, L., Hawkes, R. and Consalez, G. G. (2008). Comparative analysis of proneural gene expression in the embryonic cerebellum. *Dev. Dyn.* **237**, 1726-1735. doi:10.1002/dvdy.21571

DEVELOPMENT